# Understanding the lowering of beaches in front of coastal defence structures, Stage 2 Technical Note 9

R&D Project Record FD1927/PR9
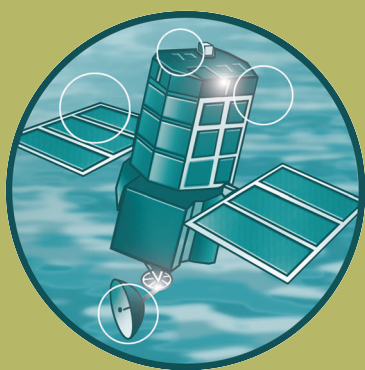
# Understanding the lowering of beaches in front of coastal defence structures, Phase 2

## Improved predictors for wave-induced scour at seawalls
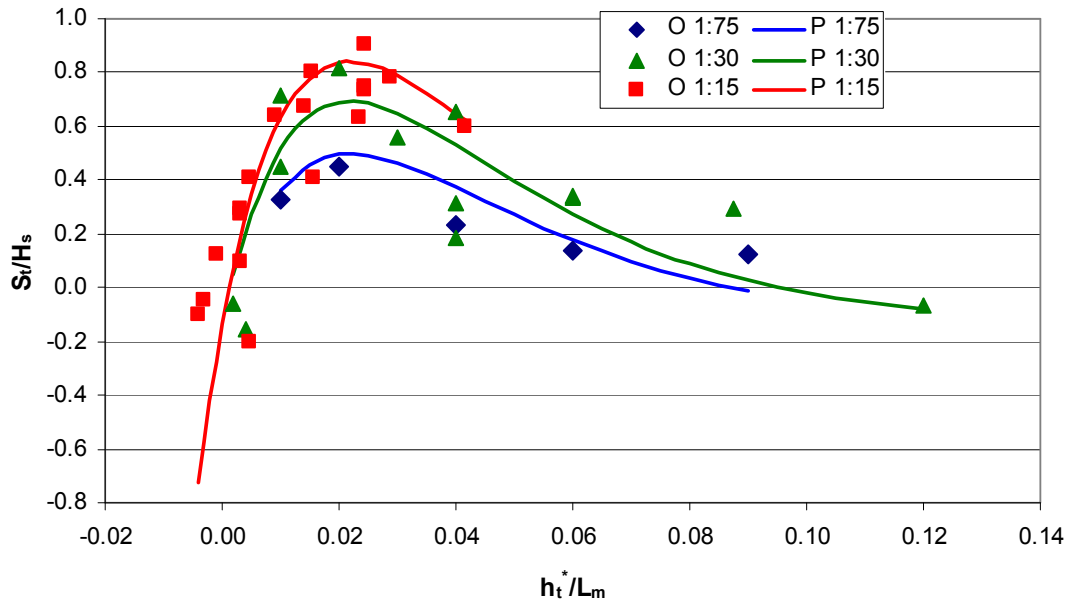


## Technical Note CBS0726/09 Release 1.0

HR Wallingford

defra
Department for Environment
Food and Rural Affairs

University
of Southampton

Understanding the lowering of beaches in front of coastal defence structures, Phase 2
Improved predictors for wave-induced scour at seawalls

HR Wallingford

# Document Information

| | |
|---|---|
| **Project** | Understanding the lowering of beaches in front of coastal defence structures, Phase 2 |
| **Technical subject** | Improved predictors for wave-induced scour at seawalls |
| **Client** | Department for Environment, Food and Rural Affairs |
| **Client Representative** | Stephen Jenkinson |
| **Project No.** | CBS 0726 |
| **Technical Note No.** | TN CBS0726/09 |
| **Filename.** | CBS0726-TN09_Improved_predictor_toe_scour_V1-0.doc |
| **Project Manager** | Dr J Sutherland |
| **Project Sponsor** | Dr RJS Whitehouse |

# Document History

| Date | Revision | Prepared | Approved | Authorised | Notes |
|---|---|---|---|---|---|
| 31/10/06 | 1.0 | Sutherland | Obhrai | Whitehouse | Issued to client representative |

Understanding the lowering of beaches in front of coastal defence structures, Phase 2
Improved predictors for wave-induced scour at seawalls

HR Wallingford

# *Contents*

Understanding the lowering of beaches in front of coastal defence structures, Phase 2
Improved predictors for wave-induced scour at seawalls

HR Wallingford

# *Contents continued*

Understanding the lowering of beaches in front of coastal defence structures, Phase 2
Improved predictors for wave-induced scour at seawalls

HR Wallingford

# 1. Introduction

This technical note describes the development of an improved predictor for the 2D cross-shore toe scour generated by waves in front of seawalls. The work was undertaken as part of the joint Defra/EA Flood and Coastal Erosion Risk Management R&D project FD1927, Understanding the Lowering of Beaches in front of Coastal Defence Structures, Stage 2. An initial scoping study (Sutherland et al., 2003, carried out as Defra/EA project FD1916) identified some shortcomings in the presently available laboratory data for scour prediction in front of seawalls and hence in the suitability of the empirical predictors of toe scour. These are summarised in Sections 1.1 and 1.2.

## 1.1 MODE OF SEDIMENT TRANSPORT

Many laboratory scour tests have been performed in relatively small wave flumes where the sediment transport was dominated by bedload transport. Examples include Sumer and Fredsøe (2000) and O'Donoghue (2001). These experimenters were well aware of the mode of sediment transport being generated and explicitly formulated empirical formulae for scour by bedload transport. However, in many cases in the field, sediment transport is dominated by suspended sediment transport. There has been a shortage of controlled laboratory experiments where suspended sediment transport has been the dominant mode of transport. This is important as the response of the beach to bedload and suspended load transport is different, as shown below.

A regular period wave reflecting off a vertical wall generates a standing wave, which in turn generates steady streaming in the thin bottom boundary layer (Longuet-Higgins, 1953). This streaming is manifested as a slow recirculating current from anti-node to node at the bottom of the bottom boundary layer and from node to antinode at the top of the bottom boundary layer. The current at the top of the boundary layer drives a counter-rotating re-circulating cell in the (much thicker) body of water above the boundary layer. This work was extended to oblique-incidence by Carter et al. (1973).

If the sediment in the bed is coarse and travels close to the bottom, it will be most influenced by the horizontal water movements in the bottom boundary layer, which are towards the node. The result is scouring midway between anti-node and node and deposition under the node (the previously-named N-type scour pattern, Xie, 1981). If the sediment is small and is maintained in suspension, it will be most influenced by the current above the bottom boundary layer, so the net movement is away from the nodes towards the antinodes producing scour under the nodes (L-type scour pattern).

Therefore the basic pattern of sediment erosion and accretion varies with the mode of sediment transport – bedload transport gives a different pattern from suspended load transport (Sumer and Fredsøe, 2002). It is important to reproduce suspended sediment transport in the laboratory experiments to provide results that are applicable in the field situation where sand is often suspended in the water column.

## 1.2 USE OF REGULAR WAVES

Many scour tests have been performed with regular period waves, rather than irregular waves with a natural spectral shape. Examples include most of the laboratory tests of Xie (1981, 1985) and Sumer and Fredsøe (2000) and all those of O'Donoghue (2001). It is not clear how to apply a scour predictor developed from regular wave laboratory experiments to a natural situation with irregular waves where wave reflections can be expected to become increasingly out of phase with distance from the wall (Hughes & Fowler, 1991).

Understanding the lowering of beaches in front of coastal defence structures, Phase 2
Improved predictors for wave-induced scour at seawalls

HR Wallingford

## 1.3   AIMS AND REPORT OUTLINE

One of the main aims of the present project was to address the deficiencies in the existing empirical scour predictors, described above.  The following steps have been undertaken in order to develop an improved scour predictor for 2D toe scour generated by waves in front of seawalls:

1. Screening of existing datasets to select only laboratory test series that generated suspended sediment transport under irregular wave conditions and collation of the chosen data (HR Wallingford, 2006a).
2. Planning of a set of medium scale laboratory flume tests to address the shortcomings in the screened datasets (HR Wallingford, 2006a).
3. Completion of a set of medium scale laboratory flume tests, including recording of bed profiles and wave conditions and the subsequent reporting of the test results (HR Wallingford, 2006b).
4. Collecting new field data at a sloping seawall at Southbourne (HR Wallingford, 2005a).
5. Re-analysing old field data at a vertical seawall in Blackpool (HR Wallingford, 2005b).

Descriptions of the data and how it was obtained are included in the referenced Technical Notes and in Sutherland et al. (2006a, 2006b) and Pearce et al. (2006).  This Technical Note summarises the data collected above and describes the steps taken to derive improved methods of scour prediction from the data.

# 2.   *Suspended sediment scour datasets*

## 2.1   XIE (1981)

Xie (1981) included a number of laboratory wave flume tests that generated scour in a flat sand bed in front of a vertical seawall in the suspension mode.  Most of the tests used regular waves but three irregular wave tests were also conducted in suspension mode.  Xie formulated an equation for the maximum scour depth over a flat bed for suspended sediment transport generated by regular waves, given in Equation 1:

$$\frac{S_{max}}{H} = \frac{0.4}{\left(\sinh kh_t\right)^{1.35}} \tag{1}$$

Where $S_{max}$ is the maximum scour depth, $H$ is the regular wave height, $k=2\pi/L$ is the wavenumber (with $L$ the wavelength) and $h_t$ is the initial water depth at the toe of the seawall.

Three irregular wave tests were conducted, although only two maximum scour depths are quoted as Xie's middle test (2c) was terminated early.  Details of the three tests are given in Table 1 and the results are plotted with Equation 1 in Figure 1, where the significant wave height, $H_s$, has been used in place of $H$ and the wavenumber, $k_p$, has been calculated at the spectral peak wave period. Note that the maximum scour depth ($S_{max}$) was at the first partial node in front of the seawall, a distance of $L_p/4$ from the seawall toe, so not at the toe, where accretion occurred.  The two irregular wave results suggest that the maximum scour depth could be predicted by a formula similar to Equation 1, but with a smaller numerator and / or a different power in the denominator.  Fitting an equation with the form of Equation 1 to the two data points gave Equation 2, which is also shown in Figure 1 but which should not be used for design as there are only two data points.

Understanding the lowering of beaches in front of coastal defence structures, Phase 2
Improved predictors for wave-induced scour at seawalls

HR Wallingford

$$\frac{S_{max}}{H_s} = \frac{0.34}{\left(\sinh k_p h_t\right)^{0.81}} \tag{2}$$

Xie's tests were conducted on a flat sand bed in relatively deep water ($h_t / H_s > 4$) so there can have been few breaking waves and little turbulence reaching the bed. The sediment transport was dominated by streaming in the recirculating cells set up in front of the seawall. The pattern of decaying accretion and scour starts with accretion at the seawall. Therefore the scour depth at the seawall, $S_t$ was negative in both cases, as shown in Table 1.

*Table 1      Xie (1981) irregular wave suspended transport scour tests*

| Test | $d_{50}$ [mm] | h [m] | $H_s$ [m] | $T_p$ [s] | $L_p$ [m] | $S_{max}$ [m] | $S_t$ [m] |
|------|------|------|------|------|------|------|------|
| 1c | 0.106 | 0.5 | 0.085 | 1.72 | 3.37 | 0.027 | -0.029 |
| 2c | 0.106 | 0.5 | 0.091 | 1.98 | 4 | - | |
| 3c | 0.106 | 0.3 | 0.071 | 1.69 | 2.7 | 0.03 | -0.039 |
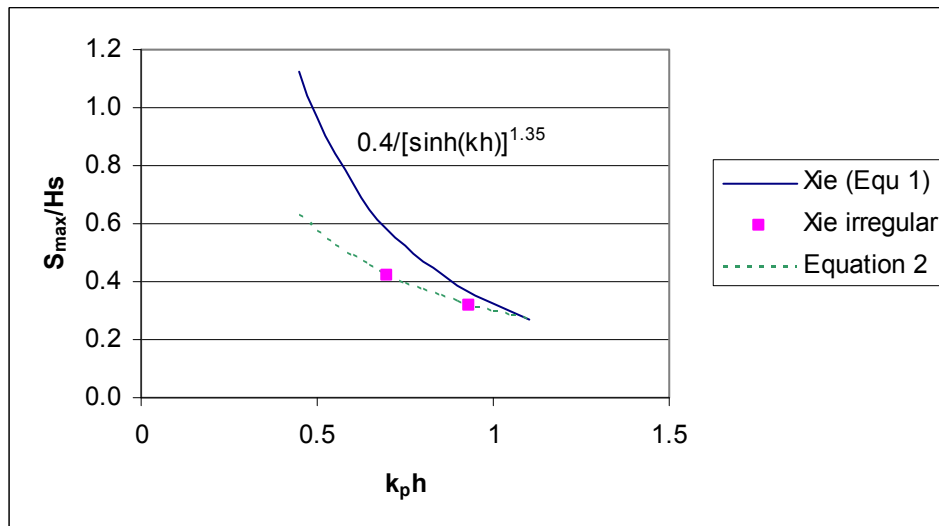


*Figure 1      Xie's (1981) regular wave best-fit maximum scour predictor, two irregular wave maximum scour depths and Equation 2 that fits the irregular wave data. Note: it is not intended that Equation 2 be used for design.*

## 2.2    FOWLER (1992)

Fowler (1992) performed mid-scale (wave heights between 0.2 and 0.3m) laboratory tests of the scouring of a 1:15 sloping sand bed in front of a vertical wall. Fowler used a scaling law to preserve the similitude of the dimensionless fall speed number between model and prototype. Results from the tests were compared with those from several previous laboratory studies and an empirical equation for scour prediction was developed in which the ratio of the depth of water at the wall to the linear theory deep-water wavelength based on the peak period was the important parameter.

Fowler's (1992) tests were valid for:
• Breaking waves
• Normally incident
• Vertical walls

Understanding the lowering of beaches in front of coastal defence structures, Phase 2
Improved predictors for wave-induced scour at seawalls

HR Wallingford

- Beach in front of structure
- Sand beach

Tests were performed within the following limits of applicability:
- $-0.011 < h_t/L_p < 0.045$ and
- $0.015 < H_s/L_p < 0.040$

Where $h_t$ = water depth at the seawall, $L_p$ = deep water linear theory wavelength at the spectral peak period, $H_s$ = deepwater linear theory spectral significant wave height.

A total of 18 irregular wave tests and 4 regular wave tests were conducted in a 100m long wave flume. Each test started with a planar beach at a slope of m=1:15. A vertical seawall was used for all tests, at a cross-shore location of $x_w$=0.9m, 0m and -0.9m where $x_w$ = 0 at the intersection of the beach and still water level and $x_w$ increases positively on moving offshore. Ottawa sand, with $d_{50}$=0.13mm and a specific gravity of 2.65 was used in all cases. Fowler (1992) used a value of $g$ = 9.844m/s$^2$ for gravitational acceleration and quoted a sediment fall speed, $w_s$ = 1.64cm/s (Fowler, 1992, p19) and $w_s$ = 1.92cm/s (Fowler, 1992, Table 1). A water temperature of 25ºC was used by him in all calculations. Waves were run for bursts of 300s and then repeated until equilibrium was established in the experiment.

The irregular wave test conditions are shown in Table 2. Here, the maximum scour depth $S_{max}$ is the maximum final bed elevation below the initial profile at cross-shore position $X_{max}$ (metres offshore from seawall). The maximum erosion depth at the seawall is denoted $S_t$.

Equation 3 shows Fowler's design relationship for maximum scour depth, $S_{max}$. Equation 3 is plotted with Fowler's irregular wave data in Figure 2. The non-dimensional ratio $S_{max}/H_s$ from Fowler (1992, Table 1 column 11) is plotted as "Fowler 1992" while the same ratio recalculated from Fowler (1992, Table 1, columns 4 and 8) is plotted as "Fowler 1992 recalculated" as there are some inconsistencies between the two versions of the same ratio. The recalculated ratios, based on quoted $H_s$ and $S_{max}$ values will be used henceforth, as given in Table 2.

$$\frac{S_{max}}{H_s} = \left(22.72\frac{h_t}{L_p} + 0.25\right)^{1/2} \tag{3}$$

Understanding the lowering of beaches in front of coastal defence structures, Phase 2
Improved predictors for wave-induced scour at seawalls

HR Wallingford

*Table 2        Summary of Fowler (1992) irregular wave test conditions*

| Test | $x_w$ (m) | $h_t$ (m) | $H_s$ (m) | $T_p$ (s) | $L_p$ (m) | $S_{max}$ (m) | $X_{max}$ (m) | $S_t$ (m) | $\dfrac{S_{max}}{H_s}$ | $\dfrac{S_t}{H_s}$ |
|------|------|--------|--------|------|--------|--------|--------|--------|--------|--------|
| S1  | 0      | 0.061  | 0.211 | 1.97 | 6.081 | 0.134 | 0.000 | 0.134  | 0.63 | 0.63  |
| S2  | 0      | 0.000  | 0.201 | 1.97 | 6.081 | 0.082 | 0.000 | 0.082  | 0.41 | 0.41  |
| S3  | 0      | 0.061  | 0.208 | 1.97 | 6.081 | 0.152 | 0.000 | 0.152  | 0.73 | 0.73  |
| S4  | 0      | 0.061  | 0.239 | 2.49 | 9.714 | 0.192 | 0.000 | 0.192  | 0.80 | 0.80  |
| S5  | 0      | -0.030 | 0.257 | 1.97 | 6.081 | 0.064 | 1.524 | 0.024  | 0.25 | 0.09  |
| S6  | 0      | -0.030 | 0.270 | 2.45 | 9.403 | 0.082 | 0.305 | 0.079  | 0.30 | 0.29  |
| S7  | 0      | -0.030 | 0.244 | 1.97 | 6.081 | 0.082 | 0.305 | 0.067  | 0.34 | 0.28  |
| S8  | 0      | 0.061  | 0.195 | 1.97 | 6.081 | 0.177 | 0.000 | 0.177  | 0.90 | 0.90  |
| S9  | 0.914  | 0.061  | 0.300 | 2.43 | 9.251 | 0.122 | 0.000 | 0.122  | 0.41 | 0.41  |
| S10 | 0.914  | 0.061  | 0.208 | 1.93 | 5.837 | 0.155 | 0.000 | 0.155  | 0.75 | 0.75  |
| S11 | 0.914  | 0.030  | 0.213 | 1.97 | 6.081 | 0.143 | 0.000 | 0.143  | 0.67 | 0.67  |
| S12 | 0.914  | 0.122  | 0.208 | 1.99 | 6.203 | 0.125 | 0.000 | 0.125  | 0.60 | 0.60  |
| S13 | 0.914  | 0.122  | 0.273 | 2.4  | 9.025 | 0.213 | 0.000 | 0.213  | 0.78 | 0.78  |
| S14 | 0.914  | 0.030  | 0.290 | 2.45 | 9.403 | 0.186 | 0.000 | 0.186  | 0.64 | 0.64  |
| S15 | -0.914 | -0.061 | 0.269 | 2.45 | 9.403 | 0.073 | 0.610 | 0.034  | 0.27 | 0.12  |
| S16 | -0.914 | -0.061 | 0.200 | 1.97 | 6.081 | 0.043 | 1.524 | -0.009 | 0.21 | -0.05 |
| S17 | -0.914 | -0.091 | 0.267 | 2.48 | 9.635 | 0.052 | 1.067 | -0.027 | 0.19 | -0.10 |
| S18 | -0.914 | 0.000  | 0.201 | 1.95 | 5.956 | 0.085 | 1.219 | -0.005 | 0.42 | -0.02 |
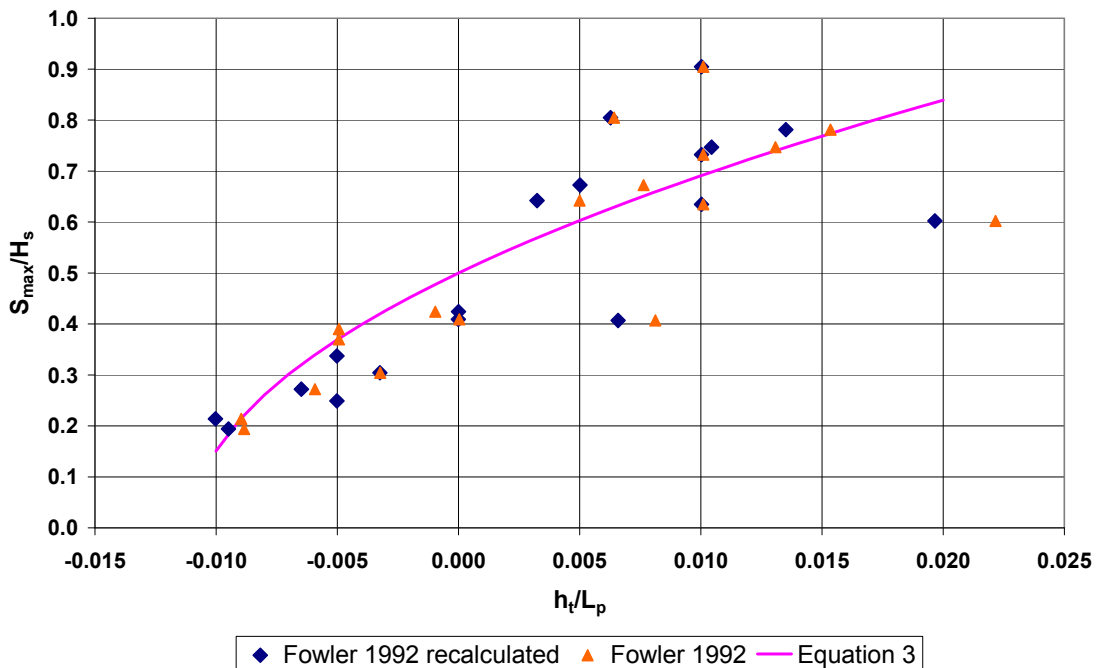


*Figure 2        Design relationship (Equation 3) and maximum scour depth data (Fowler, 1992)*

Note that in Table 2 the maximum scour depth is not always at the breakwater toe. The non-dimensional scour depth at the toe of the breakwater is plotted against $h_t/L_0$ in Figure 3. This shows a different variation of scour with relative depth and includes some negative values (i.e. accretion). The main differences between Figures 2 and 3 are for the negative values of $h_t/L_p$.

Understanding the lowering of beaches in front of coastal defence structures, Phase 2
Improved predictors for wave-induced scour at seawalls

HR Wallingford
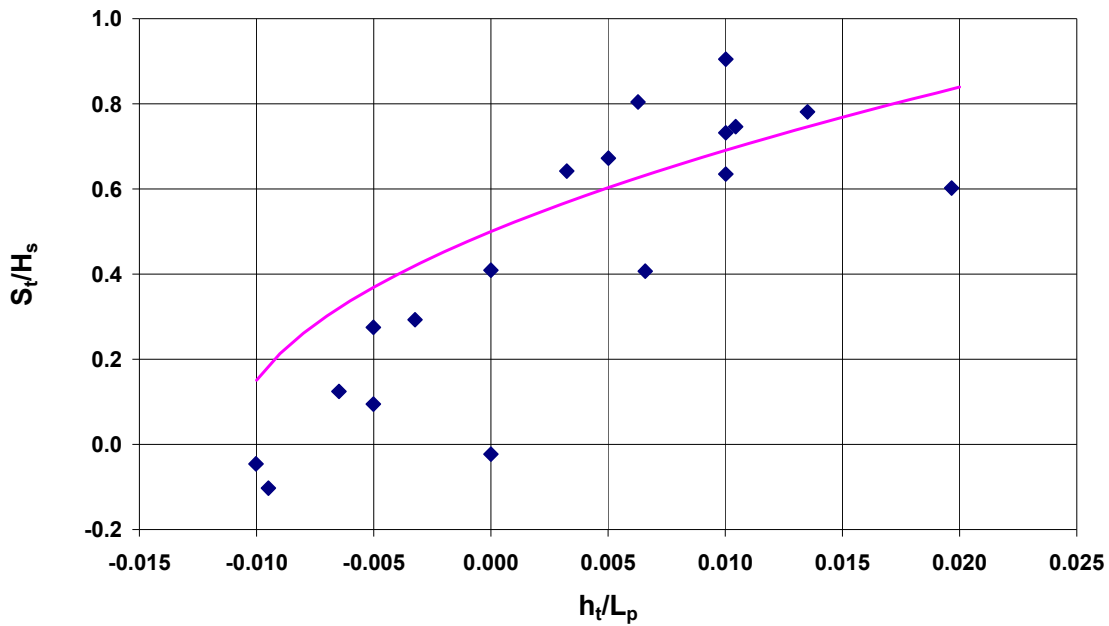


*Figure 3    Fowler's (1992) data for scour depth at the seawall toe, plus Equation 3*

Figure 4 shows Fowler's (1992) scour data plotted on the axes of a Powell and Whitehouse (1998) parametric scour plot. The numbers beside the data point are the values of $S_t/H_s$ where $S_t$ is the scour depth at the seawall and $H_s$ is the deep water incident significant wave height. The results are broadly consistent with high values to the top left of the plot and lower values to the right and negative values (accretion) towards the bottom. There are some areas where nearby $S_t/H_s$ values show considerable differences (0.91 and 0.41, for example or 0.41 and -0.02).
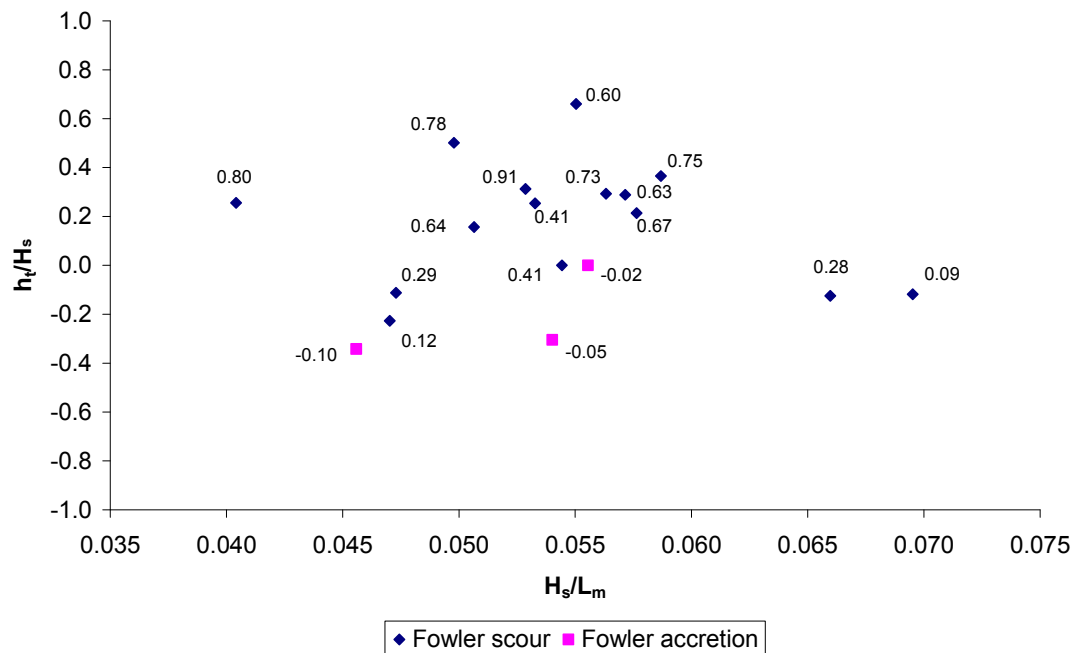


*Figure 4    Position of Fowler's (1992) irregular wave scour data on parametric scour prediction axes*

Understanding the lowering of beaches in front of coastal defence structures, Phase 2
Improved predictors for wave-induced scour at seawalls

HR Wallingford

Fowler also compared Equation 3 to data from the regular wave experiments of Barnett (1989) and Chesnutt and Schiller (1971) – where $H_0$ was taken as the wave height from the regular wave period tests. Although there was large scatter, they followed the same trend. Only irregular wave period data is considered here, so that comparison is not included.

## 2.3  HR WALLINGFORD (2006)

Tests were performed in the new 45m long wave flume at HR Wallingford and are described in HR Wallingford (2006b), Pearce et al. (2006) and Sutherland et al., (2006a, 2006b). The development of the test programme was described in HR Wallingford (2006a). The internal cross-section of the flume is 1.2m wide by 1.7m high. Waves are generated using a piston-type wavemaker with a maximum stroke of ±0.6m and a maximum operating depth of 1.4m. The wavemaker has an absorption system for absorbing wave energy reflected from the seawalls. The test setup had a 1:30 smooth concrete slope up to an elevation of 0.64m above the flume floor. The test section was a 5.14m long sand bed filled with Redhill 110 sand, which has $d_{16}$ = 0.087mm, $d_{50}$ = 0.111mm and $d_{84}$ = 0.154mm where $d_n$, is the sieve size that $n$ percent by weight of the sieved sand sample passed through. The sand bed was 0.3m deep at the offshore end. A sediment density $\rho_s$ = 2650kgm$^{-3}$ was assumed – appropriate for clean silica sand, with a $d_{50}$ settling velocity of $w_s$ = 0.86cm/s (HR Wallingford, p2, 2006b).

Tests 1 to 14 all started from a screeded 1:30 slope. The sand bed level at the wall was therefore approximately 0.80m above the flume floor (see Figure 5). Tests 15-34 started from a 1:75 screeded slope where the sand bed level at the wall was approximately 0.7m above the flume floor. Measured water temperatures were between 8.6ºC and 12.6ºC with an average of 10.8 ºC.
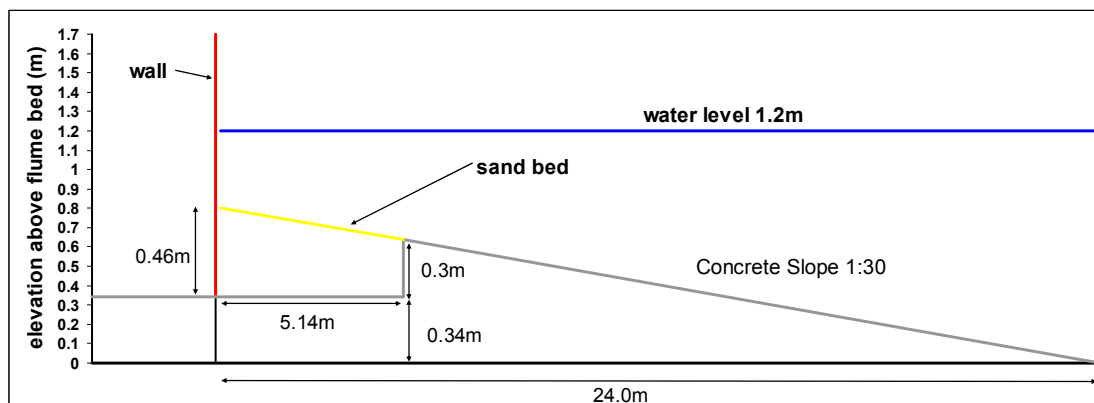


*Figure 5    Wave flume set-up*

A total of 34 tests were performed. Details of the test conditions are given in Tables 3-5, which include scour depths after N = 3,000 spectral peak wave periods.

- $H_s$ is the measured offshore significant wave height;
- $h_t$ is the still water depth at the toe of the structure;
- $T_p$ is the measured spectral peak wave period;
- $S_t$ = scour depth at seawall toe;
- $S_{max}$ = maximum scour depth;
- $X_{max}$ = Distance of $S_{max}$ from structure toe;
- $Cr$ = bulk reflection coefficient.

A total of 19 tests were performed with a smooth vertical wall, of which 13 were with a beach slope of 1:30 and 6 were with a beach slope of 1:75. Details of these are given in Table 3. A

Understanding the lowering of beaches in front of coastal defence structures, Phase 2
Improved predictors for wave-induced scour at seawalls

HR Wallingford

total of 6 scour protection tests were carried out using a vertical wall and a beach slope of 1:75. Details of these can be found in Table 4. A smooth sloping wall at 1:2 was used in 9 of the tests with a beach slope of 1:75. The wall was pivoted about the point of intersection between the beach and the wall. Details of the test conditions can be found in Table 5. The majority of tests used a constant incident significant wave height, period and depth to measure the time development of scour. However Tests 10, 17, 24, 25 and 34 were used to simulate part of a tidal cycle by running short bursts of 300 waves at different depths. Test 10 started with a water depth at the wall close to zero, increasing the depth in steps to a maximum depth of 0.3m then decreasing the depth in steps down to -0.1m at the seawall. However tests 17, 24, 25 and 34 started from a higher water depth of 0.2m and decreased the depth in steps down to -0.05m.

*Table 3      HR Wallingford (2006) vertical wall tests with no scour protection*

| Test No. | $H_s$ (m) | $T_p$ (s) | Beach slope | $h_t$ (m) | $S_t$ (m) | $S_{max}$ (m) | $X_{max}$ (m) | Cr (-) |
|---|---|---|---|---|---|---|---|---|
| HR1 | 0.193 | 1.55 | 1:30 | 0.20 | 0.057 | 0.057 | 0.031 | 0.504 |
| HR2 | 0.193 | 1.87 | 1:30 | 0.20 | 0.065 | 0.065 | 0.031 | 0.486 |
| HR3 | 0.198 | 2.29 | 1:30 | 0.20 | 0.130 | 0.130 | 0.031 | 0.467 |
| HR4 | 0.194 | 3.24 | 1:30 | 0.20 | 0.158 | 0.158 | 0.031 | 0.464 |
| HR5 | 0.197 | 4.58 | 1:30 | 0.20 | 0.140 | 0.143 | 0.049 | 0.445 |
| HR6 | 0.204 | 1.87 | 1:30 | 0.00 | -0.031 | 0.025 | 0.731 | 0.086 |
| HR7 | 0.196 | 3.24 | 1:30 | 0.00 | -0.011 | 0.032 | 1.513 | 0.133 |
| HR8 | 0.197 | 1.87 | 1:30 | 0.10 | 0.110 | 0.111 | 0.006 | 0.255 |
| HR9 | 0.202 | 1.87 | 1:30 | 0.40 | -0.013 | 0.035 | 0.327 | 0.824 |
| HR10 | 0.195 | 1.87 | 1:30 | Tidal | 0.067 | 0.067 | 0.001 | 0.308 |
| HR11 | 0.217 | 3.24 | 1:30 | 0.40 | 0.040 | 0.117 | 0.414 | 0.835 |
| HR12 | 0.197 | 3.24 | 1:30 | 0.10 | 0.088 | 0.114 | 0.469 | 0.274 |
| HR13 | 0.295 | 2.29 | 1:30 | 0.10 | 0.093 | 0.125 | 0.415 | 0.277 |
| HR14 | 0.280 | 1.87 | 1:75 | 0.30 | 0.036 | 0.052 | 0.354 | 0.488 |
| HR15 | 0.196 | 1.87 | 1:75 | 0.20 | 0.027 | 0.048 | 0.295 | 0.405 |
| HR16 | 0.197 | 3.24 | 1:75 | 0.20 | 0.089 | 0.102 | 0.404 | 0.386 |
| HR17 | 0.193 | 1.87 | 1:75 | Tidal | 0.014 | 0.034 | 0.191 | 0.156 |
| HR18 | 0.191 | 4.58 | 1:75 | 0.20 | 0.062 | 0.119 | 0.495 | 0.374 |
| HR19 | 0.215 | 3.24 | 1:75 | 0.40 | 0.050 | 0.100 | 0.417 | 0.771 |

*Table 4      HR Wallingford (2006) scour protection tests performed with a vertical wall and an initial beach slope of 1:75*

| Test No. | $H_s$ (m) | $T_p$ (s) | Beach slope | $h_t$ (m) | $S_t$ (m) | $S_{max}$ (m) | $X_{max}$ (m) | $C_r$ (-) |
|---|---|---|---|---|---|---|---|---|
| HR20 | 0.210 | 1.87 | 1:75 | 0.20 | -0.002 | 0.030 | 1.432 | 0.415 |
| HR21 | 0.196 | 3.24 | 1:75 | 0.20 | 0.006 | 0.086 | 0.713 | 0.391 |
| HR22 | 0.191 | 3.24 | 1:75 | 0.20 | 0.019 | 0.127 | 0.387 | 0.388 |
| HR23 | 0.194 | 3.24 | 1:75 | 0.20 | 0.031 | 0.125 | 0.427 | 0.298 |
| HR24 | 0.193 | 1.87 | 1:75 | 0.20 | 0.001 | 0.046 | 0.374 | 0.248 |
| HR25 | 0.199 | 3.24 | 1:75 | 0.20 | 0.010 | 0.135 | 0.231 | 0.277 |

Understanding the lowering of beaches in front of coastal defence structures, Phase 2
Improved predictors for wave-induced scour at seawalls

HR Wallingford

*Table 5     HR Wallingford (2006) sloping wall (1:2) tests all performed with a beach slope of 1:75*

| Test No. | $H_s$ (m) | $T_p$ (s) | Beach slope | $h_t$ (m) | $S_t$ (m) | $S_{max}$ (m) | $X_{max}$ (m) | $C_r$ (-) |
|---|---|---|---|---|---|---|---|---|
| HR26 | 0.190 | 1.87 | 1:75 | 0.20 | 0.063 | 0.068 | 0.165 | 0.312 |
| HR27 | 0.192 | 3.24 | 1:75 | 0.20 | 0.104 | 0.105 | 0.232 | 0.364 |
| HR28 | 0.194 | 1.55 | 1:75 | 0.20 | 0.062 | 0.072 | 0.155 | 0.283 |
| HR29 | 0.241 | 1.87 | 1:75 | 0.30 | 0.063 | 0.052 | 0.203 | 0.49 |
| HR30 | 0.243 | 3.24 | 1:75 | 0.40 | 0.043 | 0.064 | 0.124 | 0.639 |
| HR31 | 0.201 | 1.87 | 1:75 | 0.00 | -0.001 | 0.010 | 2.480 | 0.069 |
| HR32 | 0.206 | 3.24 | 1:75 | 0.00 | -0.066 | 0.023 | 2.640 | 0.118 |
| HR33 | 0.192 | 1.87 | 1:75 | 0.40 | 0.014 | 0.024 | 0.066 | 0.502 |
| HR34 | 0.200 | 3.24 | 1:75 | 0.10 | 0.069 | 0.079 | 0.201 | |
| HR34 | 0.2 | 3.24 | 1:75 | tidal | 0.074 | 0.081 | 0.210 | |

## 2.3.1  Bed level changes for a vertical wall

Bed level changes (final minus initial elevation) at the end of Tests 7, 12, 4 and 11 (i.e. after 3,000 waves) are provided in Figure 6. All the tests were performed with a vertical seawall. Negative values represent scour, while positive values represent accretion. These four tests had the same initial bed profile, wave period ($T_p$=3.24s) and incident wave height ($H_s \approx 0.2$m) but different water depths ($h_t$ = 0.0m, 0.1m, 0.2m and 0.4m respectively). A comparison has been drawn between these four tests as they resulted in very different breaking wave conditions at the wall and hence different bed profiles.

During Test 7 ($h_t$ = 0.0m) the waves broke offshore and the wave energy was largely dissipated before the waves reached the wall in the swash zone. As a result there was a slight accretion at the wall but a general lowering throughout the rest of the profile. The vertical seawall was situated within the surf zone during Test 12 ($h_t$ = 0.1m) and some breaking occurred onto it, although most of the larger waves had already broken by the time they reached the seawall. The resulting scour profile includes a small dip at the toe of the seawall caused by turbulence and a deeper scour hole at about 0.5m from the structure toe.

However during Test 4 ($h_t$ = 0.2m) the waves tended to break onto the structure and the impacts sent water high up above the seawall. In these cases water plunging down the face of the seawall to the bed resulted in suspended sediment transport at the toe and this mechanism generated the deepest scour depths. Figure 6 shows that the maximum scour occurred at the wall (0.158m) with significant accretion (0.056m) occurring 1.3m offshore.

In deeper water (Test 11, $h_t$ = 0.4m) the waves did not break onto the seawall as plunging breakers, but tended to reflect more energy. The scouring pattern (shown in Figure 6) in these cases was closer to the classic Xie (1981) standing wave pattern. The maximum scour of 0.117m occurred away from the wall and was significantly less than for Test 4, the plunging breaker case where the toe scour was 0.158m.

The presence of ripples over some parts of the test profiles indicates that the test results may be subject to some scale effects, as it is likely that under field conditions with storm waves the ripples would be washed out.

Understanding the lowering of beaches in front of coastal defence structures, Phase 2
Improved predictors for wave-induced scour at seawalls

HR Wallingford
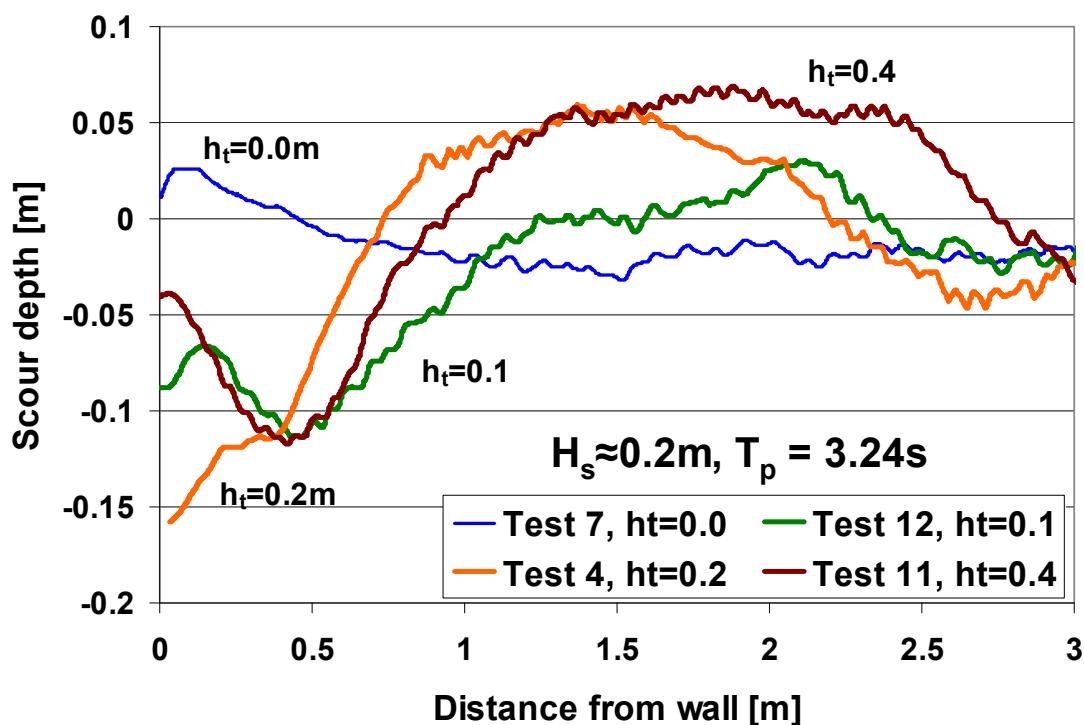
*Figure 6    Variation in final scour depth with water level for a vertical wall*

### 2.3.2   Bed level changes for a sloping wall

Bed level changes (final minus initial elevation) at the end of Tests 32, 27 and 30 (i.e. after 3,000 peak wave periods) are provided in Figure 7.  All the tests were performed with a 1:2 (V:H) smooth sloping seawall.  Negative values represent scour, while positive values represent accretion.  These three tests had the same initial bed profile, wave period ($T_p$ = 3.24s) and similar offshore incident wave height ($H_s$ = 0.19m to 0.24m) but different water depths ($h_t$ = 0.0m, 0.2m and 0.4m respectively).  A comparison has been drawn between these three tests as they resulted in very different breaking wave conditions at the wall and hence different bed profiles. In Test 27 the wave down-rush reached the sediment bed and caused the greatest scour.
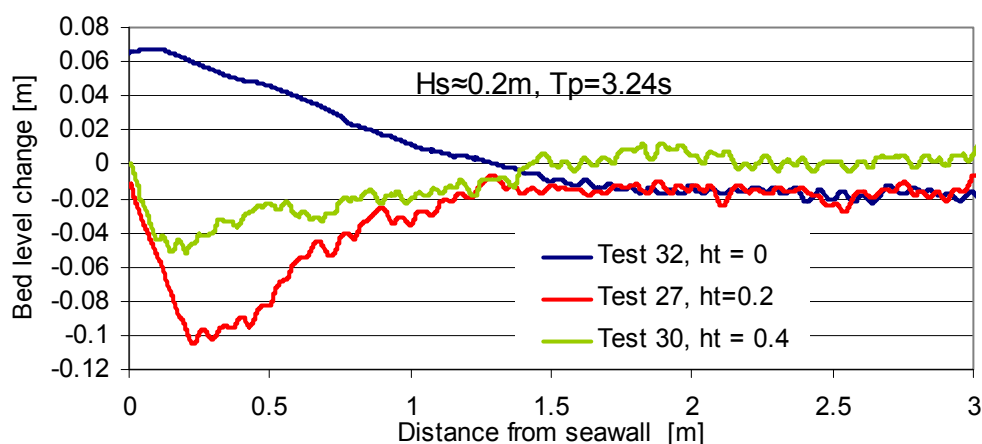


*Figure 7    Variation in final scour depth with water level for a 1:2 sloping wall*

Understanding the lowering of beaches in front of coastal defence structures, Phase 2
Improved predictors for wave-induced scour at seawalls

HR Wallingford

## 2.3.3 Effect of wall slope on scour depth

Four pairs of tests were performed where the same incident wave height, wave period and water depth were used but in the first case a vertical wall was present while in the second case a sloping wall was present. In all cases an initial bed slope of 1:75 was used. The four pairs of tests were as follows, where the average $H_s$ for both tests is given:
- 15 and 26 ($H_s = 0.20$m, $T_p = 1.87$s and $h_t = 0.20$m);
- 16 and 27 ($H_s = 0.20$m, $T_p = 3.24$s and $h_t = 0.20$m);
- 14 and 29 ($H_s = 0.26$m, $T_p = 1.87$s and $h_t = 0.30$m);
- 19 and 30 ($H_s = 0.23$m, $T_p = 3.24$s and $h_t = 0.40$m).

The sloping wall scour depth is plotted against the vertical wall scour depth in Figure 8, for the scour depth at the structure toe and the maximum scour depth. The diagonal line plotted is the line of equivalence. Figure 8 shows that for the four cases tested the scour depths were not, on average, reduced by replacing a vertical seawall with a 1:2 sloping seawall. This runs contrary to many people's expectations that reducing the wall slope reduces the scour depth as it reduces the reflection coefficient.

As with a vertical wall the scour depth reached partly depends on the way the wave runs down the seawall slope and interacts with the following wave. Deep scour depths appear to correlate well with wave run-down reaching the structure toe, which continued as a 1:2 slope under the beach in these tests.
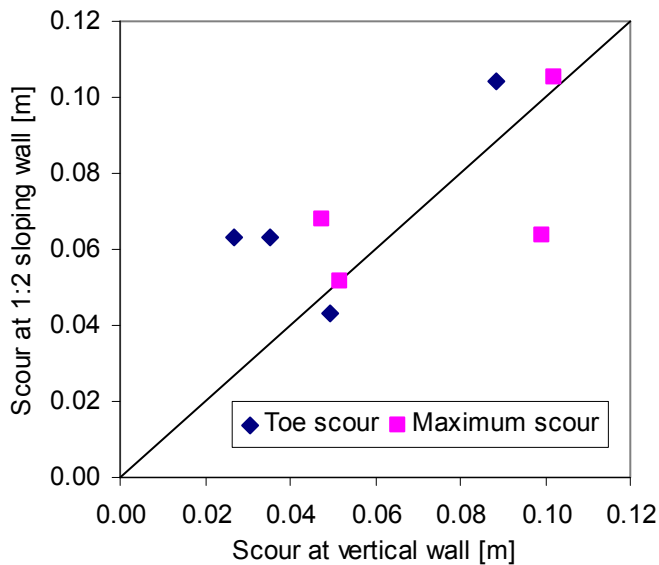


*Figure 8      Comparison between scour depths at a 1:2 and a vertical seawall*

## 2.3.4 Effect of beach slope on scour depth

Four pairs of tests were performed where the same incident wave height, wave period, water depth and structure were used but in the first case the initial beach profile was at 1:30 while in the second case the initial beach slope was 1:75. The four pairs of tests were as follows, where the average $H_s$ for both tests is given:
- 2 and 15 ($H_s=0.19$m, $T_p=1.87$s and $h_t=0.20$m);
- 4 and 16 ($H_s=0.20$m, $T_p=3.24$s and $h_t=0.20$m);
- 5 and 18 ($H_s=0.19$m, $T_p=4.58$s and $h_t=0.20$m);

Understanding the lowering of beaches in front of coastal defence structures, Phase 2
Improved predictors for wave-induced scour at seawalls

HR Wallingford

- 11 and 19 ($H_s$=0.22m, $T_p$=3.24s and $h_t$=0.40m).

The scour depths for the 1:75 beach slope are plotted against the scour depths for the 1:30 beach in Figure 9, which shows the toe scour depths and the maximum scour depths. It is clear that the 1:75 beach slope gave much lower scour depths than the 1:30 beach slope. Best-fit straight lines through the origin gave toe scour depths in the 1:75 beach as 52% of those in the 1:30 beach, while maximum scour depths were 75% of those in the 1:30 beach. The reason for this is considered to lie in the way the waves broke on the beach in front of the seawall.

The waves tended to break as spilling breakers on the 1:75 beach, whereas for the 1:30 case there were more breakers plunging onto the seawall causing turbulent jets to reach the seabed, resulting in scour.
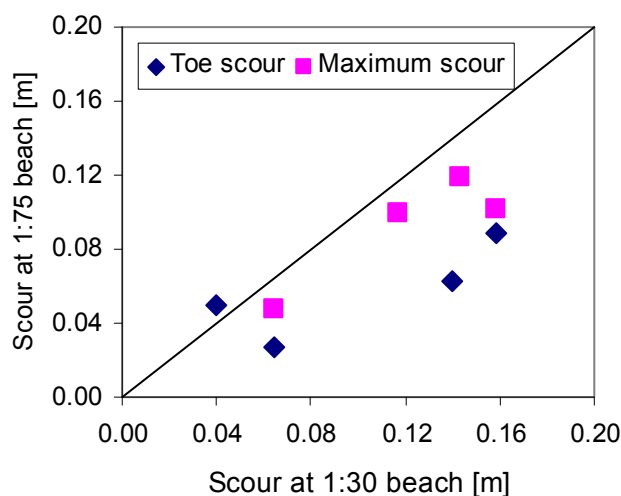


*Figure 9      Scour depth at 1:75 beach against scour depth at 1:30 beach*

### 2.3.5  Variation in scour depth with relative water depth

Figures 10 and 11 show the variation of relative scour depth, $S/H_s$ with relative toe depth, $h_t/L_p$ where $L_p = gT_p^2/(2\pi)$ is the deep water linear theory wavelength for the wave peak period, $T_p$. Throughout, it has been assumed that the average wave period, $T_m = 0.781 \times T_p$ as JONSWAP spectra with standard parameters were used (Soulsby, 1997) so the deep water linear theory wavelength for the average period, $T_m$, is given by $L_m = gT_m^2/(2\pi) = 0.781^2 L_p = 0.61 L_p$. Figure 10 shows the scour depth at the toe, $S_t/H_{si}$ while Figure 11 shows the relative maximum scour depth, $S_{max}/H_{si}$. In the legends V denotes a vertical wall and S the 1:2 smooth sloping wall; 1:30 and 1:75 denote the original beach slopes. Figures 10 and 11 show the highest relative scour depths occurring for relative toe depths of $h_t/L_p \approx 0.01$ in both cases.

Understanding the lowering of beaches in front of coastal defence structures, Phase 2
Improved predictors for wave-induced scour at seawalls

HR Wallingford
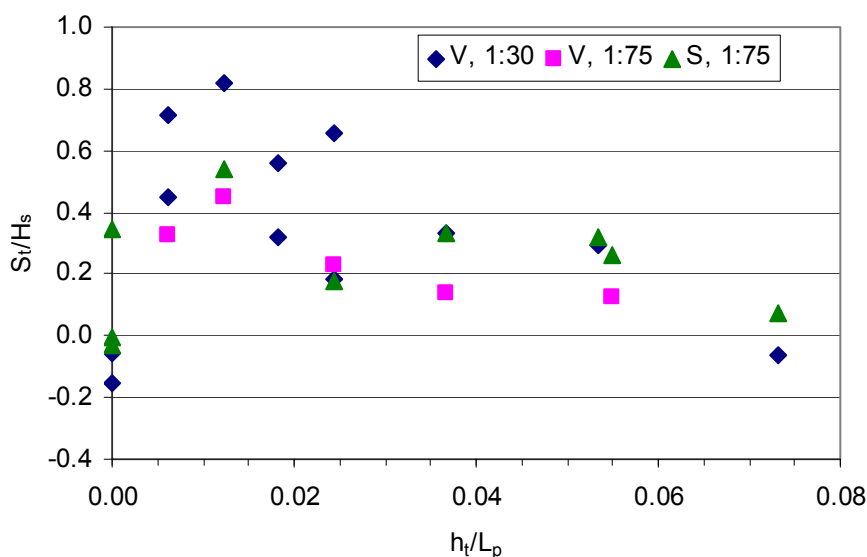
*Figure 10    Variation in toe scour depth with relative water depth*
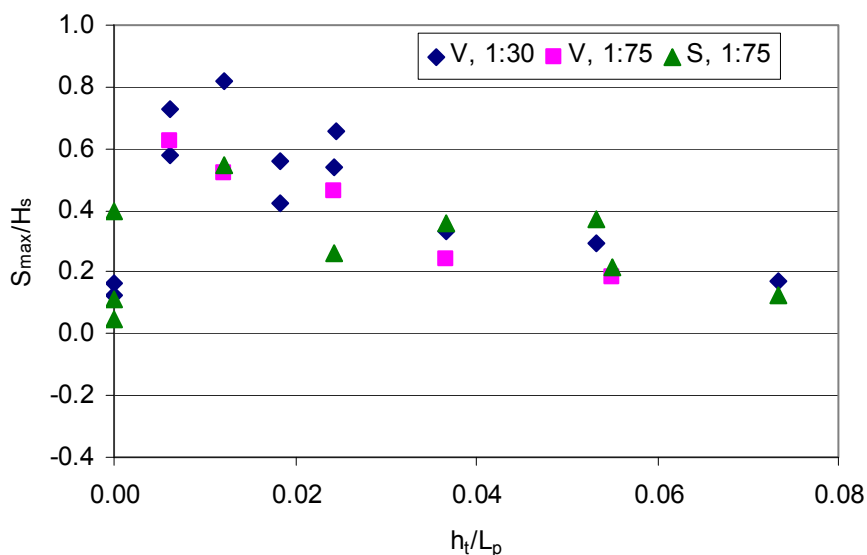


*Figure 11    Variation in maximum scour depth with relative water depth*

The trend of decreasing relative scour depths with increasing relative depth (for $h_t/L_p > 0.012$) fits with the form of the scour prediction formulae devised by Sumer and Fredsøe (2000) and Xie (1981) where measurements were made within this range.  The trend of increasing relative scour depths for increasing relative depth (for $h_t/L_p < 0.012$) fits with the form of the scour prediction formulae devised by Fowler (1992) whose experiments showed increasing relative scour depths for $h_t/L_p \leq 0.015$.  Some authors, such as McDougal et al. (1986) had considered that the variation of scour depth with relative depth in Fowler (1992) ran contrary to expectations and other scour formulae.

These tests have reproduced the form of the results in Fowler (1992) within the expected range. This illustrates the fact that scour occurs by different mechanisms in different hydrodynamic

Understanding the lowering of beaches in front of coastal defence structures, Phase 2
Improved predictors for wave-induced scour at seawalls

HR Wallingford

regimes. The different scouring mechanisms should not be expected to exhibit the same variation in scour depth with relative water depth. These tests have helped to reconcile the approaches of Fowler (1992), Xie (1981) and Sumer and Fredsøe (2000).

Figure 10 shows that accretion occurred at the structure toe for the lowest and in one case for the highest relative water depths. Accretion occurred at the toe of the vertical structure for $h_t/L_p \approx 0$ due to swash zone processes. At high relative depths the lack of wave breaking resulted in scouring patterns dominated by streaming and therefore similar in form to those in Xie (1981). In these cases accretion at the toe of the structure can occur.

Figures 10 and 11 illustrates the differences between maximum and toe scour depths. Maximum scour depths are all positive and are always larger than or equal to the toe scour depth. The maximum value of relative scour depth recorded was $S/H_s = 0.82$ (for Test HR4, Table 2).

### 2.3.6 *Variation in scour depth with Iribarren number*

The observed dependency of the scour depth on the form of wave breaking on the structure indicates that there might be a relationship between scour depth and the Iribarren number (Battjes, 1974) or surf similarity parameter as it is also known defined in Equation 4 and including the beach slope, $\tan(\alpha)$.

$$Ir = \frac{\tan(\alpha)}{\sqrt{H_{si}/L_p}}$$

(4)

On a uniformly sloping beach without a seawall the breaker type has been categorized as spilling for $Ir < 0.5$ and plunging for $0.5 < Ir < 3.3$ (Smith, 2003) although there is no abrupt limit from one breaking state to the other for irregular waves. In this case the wave breaking in front of the structure was heavily influenced by the reflections from the structure, with reflection coefficients in excess of 0.8 (see Tables 3 to 5). This has resulted in waves plunging onto the seawall for Iribarren numbers less than 0.5. Figures 12 and 13 show the variation of relative scour depth with Iribarren number for toe scour and maximum scour.
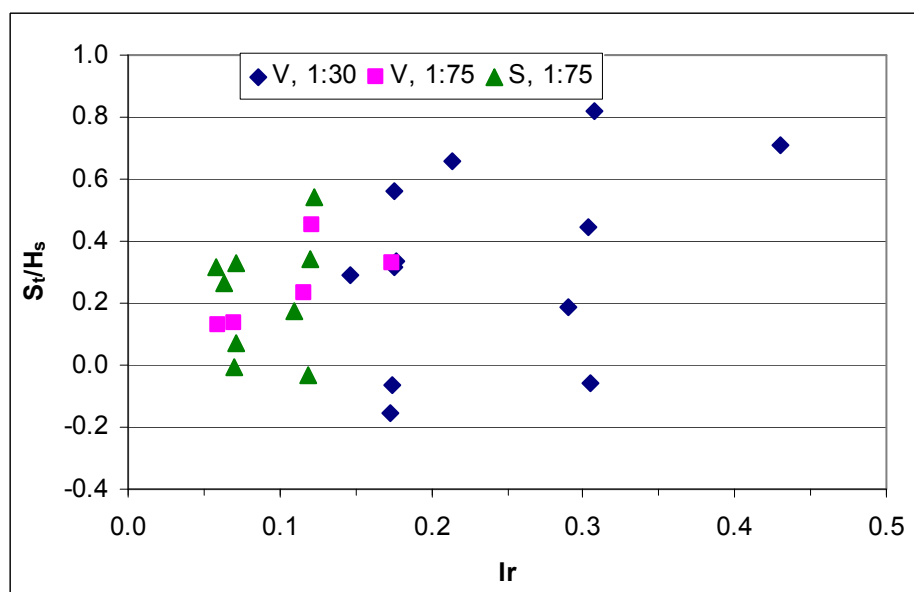


*Figure 12    Variation in toe scour depth with Iribarren number*

Understanding the lowering of beaches in front of coastal defence structures, Phase 2
Improved predictors for wave-induced scour at seawalls

HR Wallingford
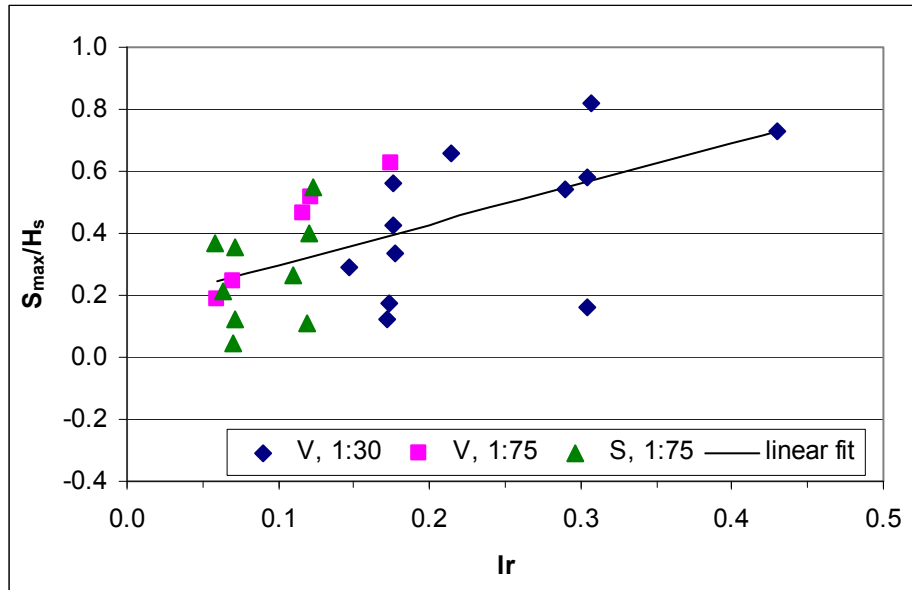


*Figure 13   Variation in maximum scour depth with Iribarren number; linear fit is given by Equation 5*

There is a stronger apparent link between the relative maximum scour depth and Iribarren number than there is between the toe scour depth and the Iribarren number. A number of simple best-fit curves were calculated to show the link between relative maximum scour depth and Iribarren number. The simple linear fit given in Equation 5 had the equal lowest mean absolute error of 0.13.

$$\frac{S_{max}}{H_s} = 1.30 \times Ir + 0.169 \qquad\qquad (5)$$

However, there is a considerable variation in scour depths for similar values of Iribarren number. For example Tests 4, 7, 11 and 12 all have Iribarren numbers between 0.29 and 0.31 but have relative maximum scour depths between 0.16 and 0.82. All four tests have incident significant wave heights between 0.194m and 0.217m, peak periods of 3.24s and were performed with a vertical seawall and an initial beach slope of 1:30. The difference lies in the toe depth, which governs where the seawall is in relation to the position waves start to break and hence which hydrodynamic processes dominated. See Section 2.3.1 for a discussion of these tests and Figure 6 for their final bed profiles.

### 2.3.7 Variation in relative scour depth with Iribarren number and relative toe depth

Sections 2.3.5 and 2.3.6 have shown how scour depths vary with relative depth and Iribarren number respectively. Figure 14 shows the relative toe scour depth plotted against the relative toe depth, while Figure 15 shows the relative maximum scour depth plotted against the relative toe depth. In both cases the data was arranged into three ranges of Iribarren number:
- $Ir < 0.08$;
- $0.1 < Ir < 0.2$; and
- $Ir > 0.2$.

Figures 14 and 15 show that for any given relative depth, $h_t/L_p$, the greatest scour depths tend to occur for the larger Iribarren numbers. The trend appears more visibly obvious for the

Understanding the lowering of beaches in front of coastal defence structures, Phase 2
Improved predictors for wave-induced scour at seawalls

HR Wallingford

maximum scour depth than for the toe scour depth.  This opens up the possibility of developing a scour predictor that is a function of relative toe depth and Iribarren number.
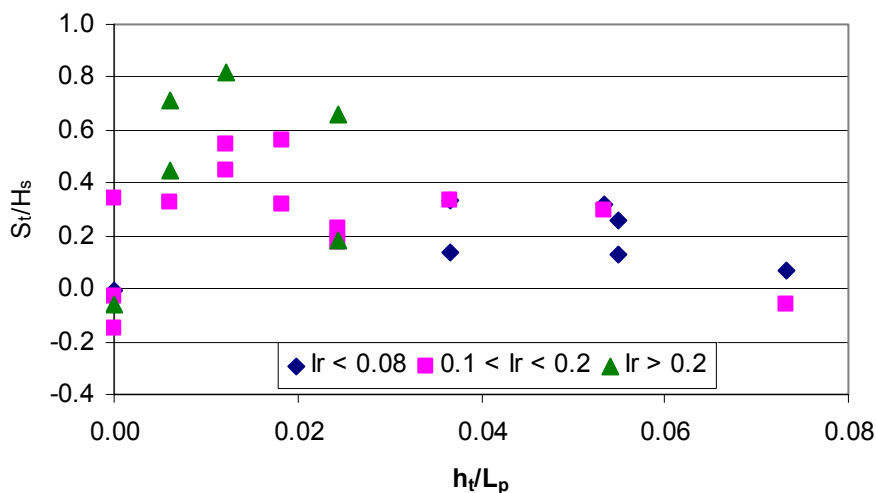


*Figure 14    Variation in toe scour depth with depth for ranges of Iribarren number*
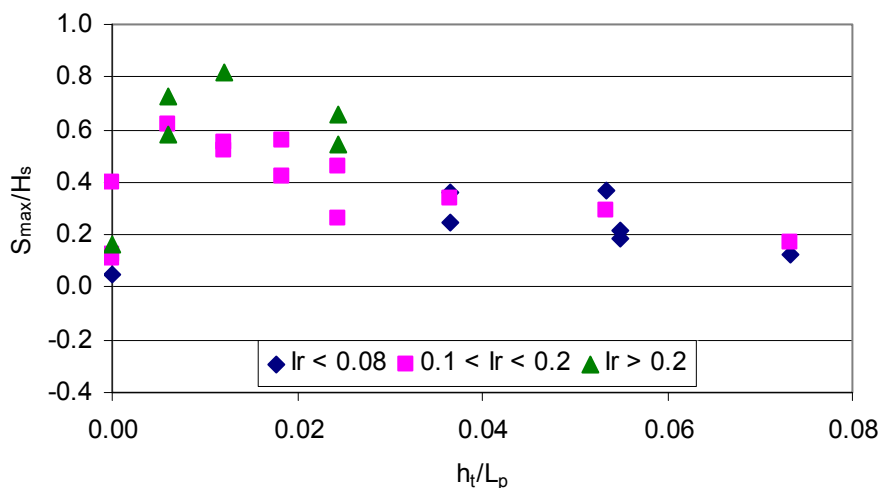


*Figure 15    Variation in max scour depth with depth for ranges of Iribarren number*

## 2.3.8  Ranges of tests and limits to scour depth

The tests performed at HR Wallingford were within the following ranges:

- $0.000 \leq h_t/L_p \leq 0.073$;
- $0.059 \leq Ir \leq 0.430$;
- $0.00 \leq h_t/H_s \leq 2.08$;
- $0.006 \leq H_s/L_p \leq 0.052$;

Moreover, not all sections of these ranges were covered equally.  Therefore, as with any set of experimental results, any extrapolation outside these limits (and for some cases within these

Understanding the lowering of beaches in front of coastal defence structures, Phase 2
Improved predictors for wave-induced scour at seawalls

HR Wallingford

limits) carries a risk. Nevertheless, some limits can be placed on the expected behaviour due to our understanding of the physical processes involved.

If the beach extends above the maximum runup limit for a particular seastate, the waves will not reach the seawall so the scour depth at the wall is expected to be zero. Note however, that wave activity seawards of the beach toe may cause erosion that may, in time, extend to the seawall toe. At the other extreme of very deep water the wave orbital velocity will tend towards zero and again no scour would be expected to occur. For relatively deep water and low (or flat) bed slopes accretion also occurs at the seawall toe for suspended load sediment transport, as shown by test HR9, see Table 3, and by Xie (1981), see Table 1.

## 2.3.9 Modelling of a half tidal cycle

Measurements of toe scour at seawalls in the inter-tidal zone (Pearce et al., 2006) show that scour holes can often form and refill within a single tide, leaving the beach level after the event similar to, or the same as, the beach level before the event. The full extent of such events cannot be determined from beach profiles measured at low tide.

Test 10 modelled a half tidal cycle using bursts of 300 peak wave periods at a series of discrete water levels, starting at 0.05m above the intersection of the vertical seawall and the initial 1:30 bed profile. The water level was then increased in steps of 0.05m to 0.30m before decreasing in steps of 0.05m to a level of -0.10m. Two additional bursts were then added, at levels of -0.08m and -0.09m to see if more infilling of the scour hole would occur.

The same offshore wave conditions were used for all water levels, with a target significant wave height of 0.20m, and spectral peak period of $T_p = 1.87s$. The gains on the wavemaker and the wave absorption system were tuned to the water depth before running each burst of waves to ensure that the offshore wave conditions were as uniform as possible. The bed profiles from Test 10 are shown in Figure 16, which is split into three sections.

Figure 16a shows the bed levels profiles from the rising water levels. The scour depth at the wall increased up until 1200 waves (with a water depth at the toe of 0.20m above the initial bed level) then decreased as the water level rose to 0.30m after 1800 waves. This is compatible with the results from Section 2.3.5 and the observations that the greatest scour depths are achieved when waves break directly onto the seawall. This was observed to occur more at a depth of 0.20m than at higher or lower depths. The position of the maximum accretion (within 1.5m of the seawall) moves offshore from the seawall as the water depth and hence wavelength increases.

Figure 16b shows the bed profiles from the greatest water depth of 0.30m (the last profile shown in Figure 16a) down to a depth of 0.05m, after 3300 peak wave periods. Here the scour depth at the wall did not increase noticeably as the water level dropped from 0.30m to 0.20m, but it did increase as the water depth dropped from 0.20m to 0.10m. At the same time the location of maximum accretion (within 1.5m of the seawall) moved towards the seawall and decreased in elevation as the water level dropped, until after 3300 waves there was no accretion within 1.5m of the wall and the whole section of the seabed exhibited erosion. Between about 2m and 3m offshore a second area of accretion remained above the initial bed level.

Understanding the lowering of beaches in front of coastal defence structures, Phase 2
Improved predictors for wave-induced scour at seawalls

HR Wallingford
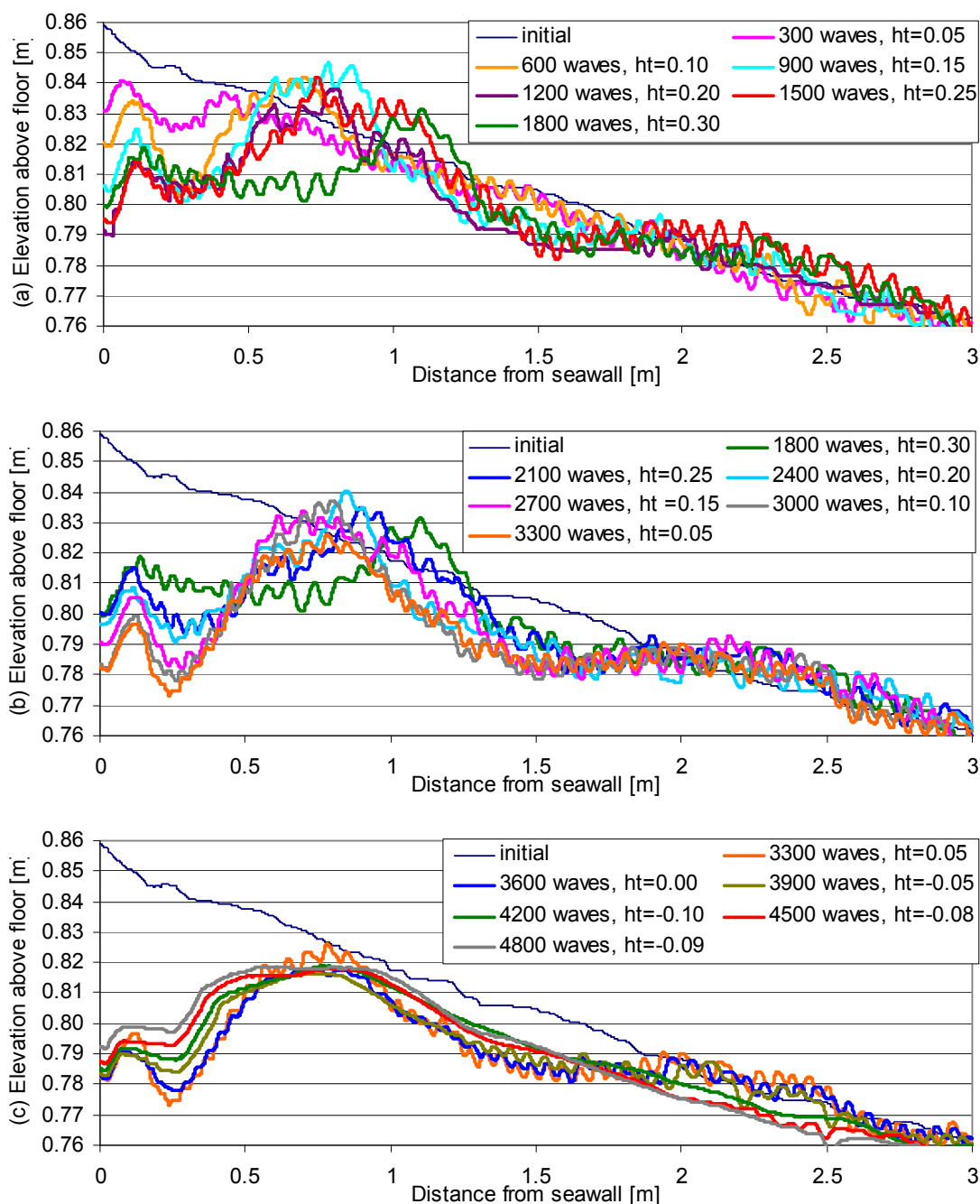


*Figure 16   Bed levels measured every 300 waves for a half tidal cycle; (a) rising water level, (b) falling water level and (c) further decrease in water level*

Figure 16c shows the scour profiles from a water depth of 0.05m down to -0.10m then after 2 further bursts of waves at -0.08m and -0.09m. At these low water levels the further offshore mound (between 2m and 3m from the seawall) became gradually washed out and the bed profiles became smoother. The toe scour in front of the seawall also started to fill in by a small amount. The water depths for the final two bursts were chosen so that the offshore mound was just exposed as it seemed to be periodic swash events over this outer mound that contributed most to the infilling.

Understanding the lowering of beaches in front of coastal defence structures, Phase 2
Improved predictors for wave-induced scour at seawalls

HR Wallingford

Figure 16c shows that the nearly complete infilling of scour holes seen in the field (Pearce et al., 2006) was only partially reproduced in the medium scale laboratory tests. Scale effects and the discrete representation of changes in water level as well as the longshore uniformity of bed levels in the flume are all likely to have contributed to the differences between the results in the laboratory and measurements made in the field.

### 2.3.10 Summary of HR Wallingford scour tests

A set of thirty-four medium-scale laboratory tests of toe scour at seawalls has been performed. The tests were all intended to generate suspended sediment transport within the laboratory flume and suspension was often observed during the tests. The tests were all carried out with irregular waves. The results are complementary to other laboratory tests that also used irregular waves, particularly 2 tests of Xie (1981), 1 of Kraus and Smith (1994) and 18 of Fowler (1992).

Two scour depths were determined: $S_t$ the scour depth immediately adjacent to the toe of the structure and $S_{max}$ the maximum scour depth measured at any point in the test section. Both are of interest in considering the stability of coastal structures. The presence of a deep scour hole at the toe of a structure may allow fill material to escape under the seawall, leaving a void behind the seawall that may cause its sudden collapse. A deep scour hole at the toe of the structure also means that the toe may slide outwards – another form of failure. A scour hole away from the structure toe is also of interest as its presence may shorten any slip surface, thereby increasing the likelihood of structural failure by sliding.

The relative scour depth was found to depend on the relative water depth at the structure toe, $h_t/L_p$ and the Iribarren number. It was relatively insensitive to the slope of the seawall, with a smooth 1:2 slope giving similar scour depths to a vertical seawall.

An attempt was made to reproduce the formation and in-filling of a scour hole during a half tidal cycle, as observed in the field. Only partial infilling occurred, probably as a result of scale effects and the discrete changes in water level made during the test.

## 3. Combined dataset comparisons

### 3.1 COMPARISON WITH FOWLER AND XIE

Two of the most often quoted scour predictors are those of Fowler (1992) given in Equation 3 and Xie (1981) given as Equation 1, which are plotted in Figure 17 recast in terms of $h_t/L_m$ rather than the original $k_p h_t$. Figure 17 has the form of Figure 8.11 in Sumer and Fredsøe (2002) recast in terms of $h_t/L_m$. In addition the experimental data from the HR Wallingford test results are also shown with the results from Fowler (1992), the Supertank experiment (Kraus and Smith, 1994) and Xie (1981). Figure 17 shows that the Fowler curve generally over predicts the measured scour for low relative depths (which is the range it is calibrated for) while Sumer and Fredsøe (2000) significantly over predicts the scour depths at relatively high water depths (which is the range it was calibrated for). The latter is to be expected as Sumer and Fredsøe (2000) generally used regular waves and noted that scour depths for irregular waves were considerably lower.
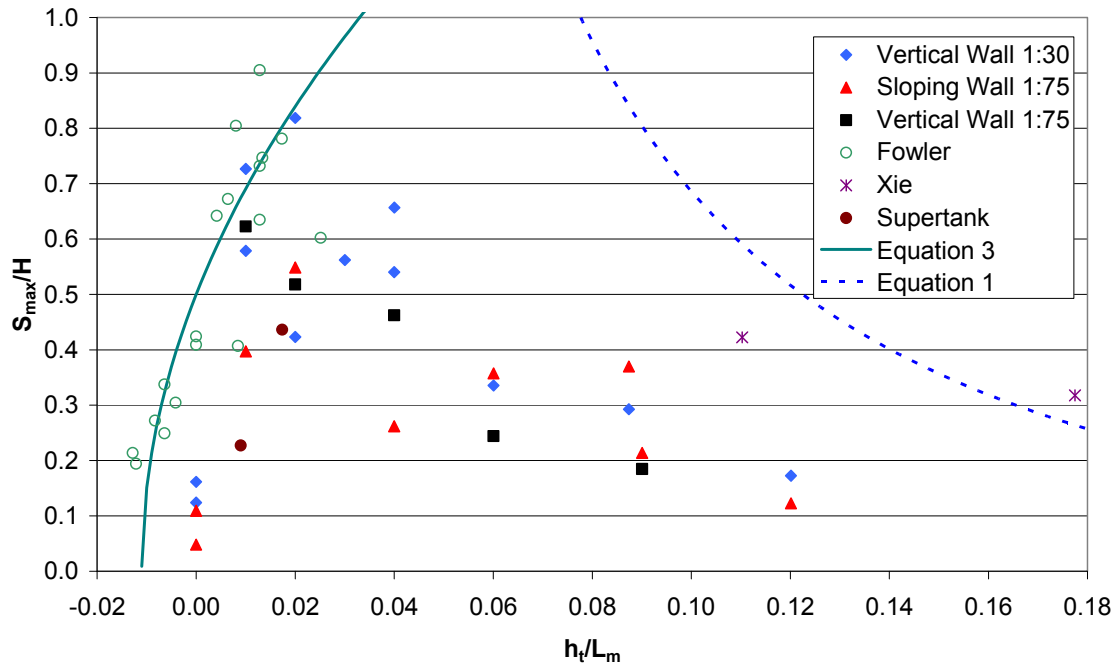
*Figure 17    Experimental results plotted against prediction curves of Fowler (Equation 3) and Xie (Equation 1)*


## 3.2    PARAMETERIC SCOUR PLOT

The combined dataset is presented as a parametric scour plot, of the form derived by Powell and Lowe (1994) and Powell and Whitehouse (1998) for shingle and sand, respectively.   In a parametric plot the axes are $h_t/H_s$ (which takes the form of an inverted wave breaking criterion) and $H_s/L_m$ (which is a measure of the deep water wave steepness).   The combined dataset is shown in Figure 18, where different symbols represent the different ranges of $S_t/H_s$.   The results show that there are distinct areas with relatively high scour depth and areas with relatively low scour depths, implying that a contouring exercise could be carried out based on the data.   The original parametric scour plot for sandy seabeds, given in Powell and Whitehouse (1998) is reproduced as Figure 19.

Understanding the lowering of beaches in front of coastal defence structures, Phase 2
Improved predictors for wave-induced scour at seawalls

HR Wallingford
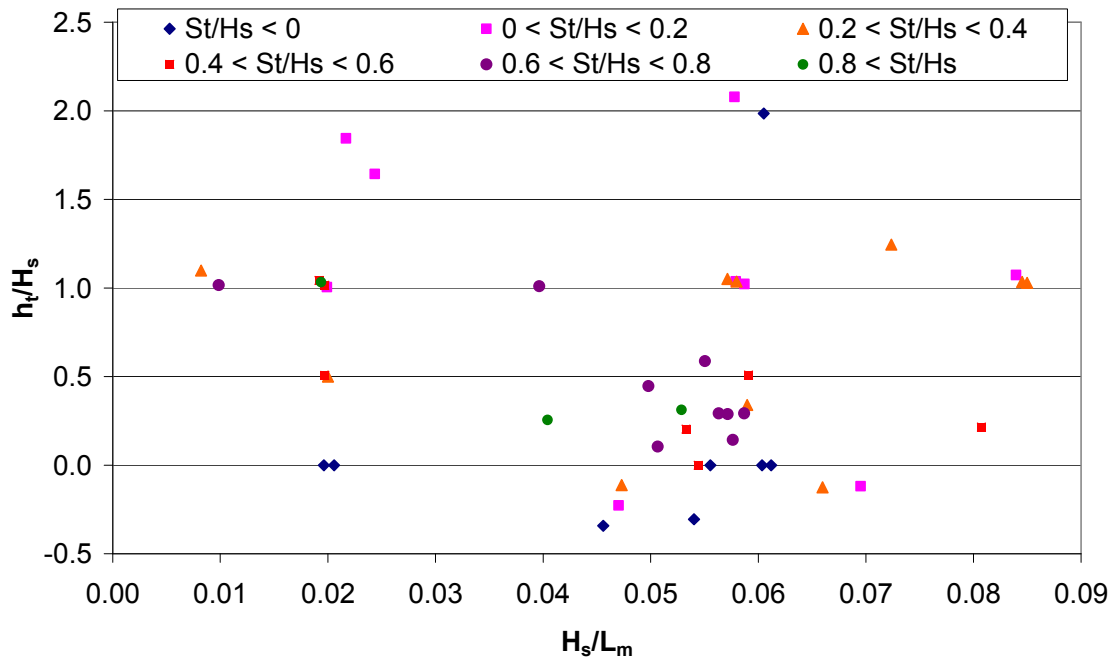
*Figure 18    Combined dataset plotted as a parametric scour plot*
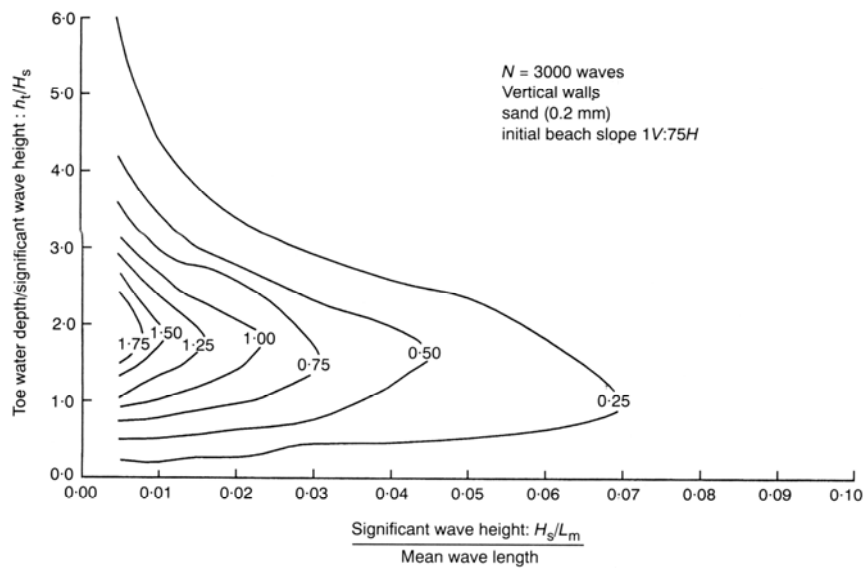


*Figure 19    Powell and Whitehouse (1998) parametric scour plot showing contours of St/Hs*

Figure 19 was derived from the use of a calibrated COSMOS 2DV cross-shore numerical model.  The data in Figure 18 correspond to some extent with Figure 19, but there are higher measured scour depths for storm waves with $0.04 < H_s/L_m < 0.06$ that occur for lower relative depths ($h_t/H_s < 0.5$) than shown in Figure 19.  In general the highest scour depths were measured at lower relative depths than given in Figure 19.

Multiplying the parametric scour plot axes together gives the relative depth: $h_t/H_s \times H_s/L_m = h_t/L_m$.  Therefore it is possible to draw contours of equal value of $h_t/L_m$ on a

Understanding the lowering of beaches in front of coastal defence structures, Phase 2
Improved predictors for wave-induced scour at seawalls

HR Wallingford

parametric scour plot, as shown in Figure 20, where $h_t/L_m$ values of 0.001, 0.016 and 0.06 have been plotted.
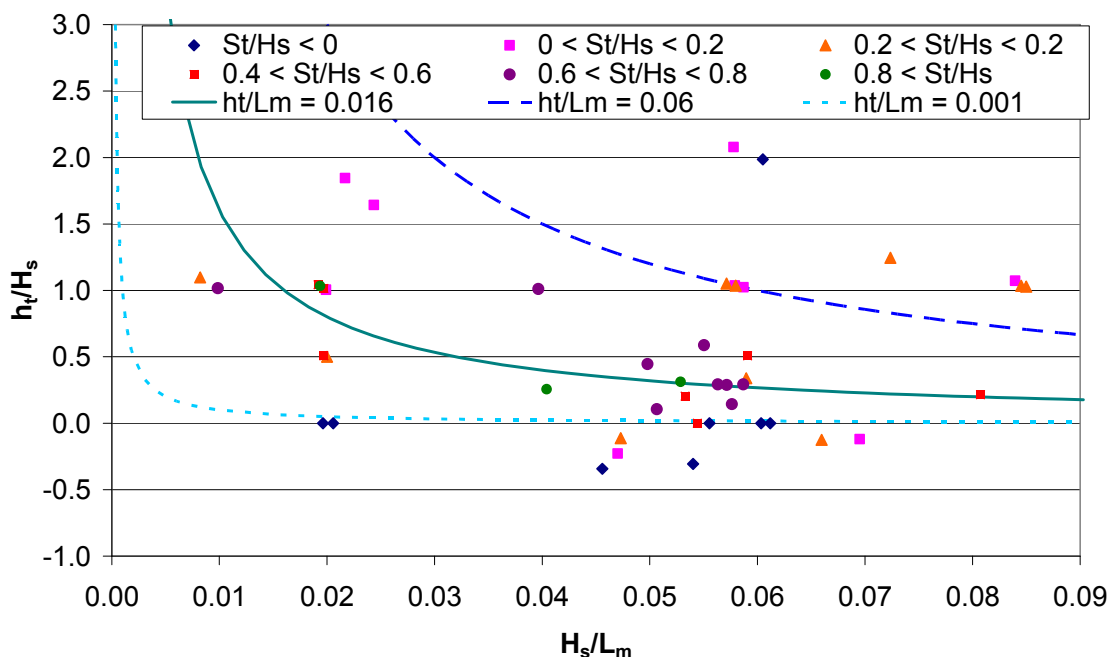


*Figure 20    Parametric scour plot with contours of equal $h_t/L_m$*

The approach of fitting scour depths as a function of relative depth, $h_t/L_m$ implies that all situations with the same $h_t/L_m$ should have the same relative scour depths, $S/H_s$. It follows that all points on the $h_t/L_m$ contours plotted on Figure 20 should have the same relative scour depth. The same contour goes from a high offshore steepness wave in lower depth/wave height region to a lower steepness wave in a higher depth/height region.   The $h_t/L_m = 0.016$ value (which is approximately at the peak of the data in Figure 17) goes from low steepness non-breaking waves to high steepness breaking waves.  This indicates why some of the scatter in the relative scour versus relative depth graphs occurs and shows that the best form of scour predictor would include more parameters than just relative depth.

# 4. Improved scour predictors as functions of relative depth

The improved scour predictors in Sections 4.2 to 4.5 have been developed at the University of Southampton (UoS) by Andrew Pearce as part of his PhD thesis.  The data used was from the Fowler (1992) and HR Wallingford (2006b) tests with a vertical seawall.  The approach used was developed by Andrew Pearce with Dr James Sutherland (HRW) and Dr Gerald Müller (UoS).  In each case the data was split into two ranges representing (i) increasing and (ii) decreasing relative scour depth with increasing relative toe depth.  Separate equations for relative scour depth as a function of relative toe depth were fitted to high and low ranges and a range of error statistics was calculated for each case.  The value of the breakpoint was varied as was the form of equation fitted to find the pair of equations and the value of the breakpoint that gave the lowest overall Root-Mean-Square Error (RMSE).

Understanding the lowering of beaches in front of coastal defence structures, Phase 2
Improved predictors for wave-induced scour at seawalls

HR Wallingford

The improved scour predictors in Sections 4.6 to 4.7 were developed by Dr James Sutherland at HRW.

The first part of this section describes the statistics used to judge the best fit and subsequent sections look at best-fit equations for toe scour and maximum scour, firstly using four fitted variables for each of the ranges then using a simplified set of equations. A conservative predictor for toe scour depth was then derived, followed by a single equation for toe scour depth over the full range of relative depths.

## 4.1 STATISTICS BASED ON AVERAGE, VARIANCE AND ROOT-MEAN-SQUARE

The mean and standard deviation of a set of results are (normally) useful measures of central tendency and the variation about it. Let the average of a set, $X$, of N results be given by $<X>$. Similarly, let the average of a set Y of N corresponding predictions be given by $<Y>$.

In assessing a predictive model, knowledge of the difference between measured and predicted sets of results is essential. The simplest measure of the difference is the bias:

$$Bias = \langle Y \rangle - \langle X \rangle \tag{6}$$

The variation of the sets X and Y about their means are characterised by their variances ($\sigma_X^2$ and $\sigma_Y^2$) and standard deviations ($\sigma_X$ and $\sigma_Y$) given by:

$$\sigma_X^2 = \left\langle \left( X - \langle X \rangle \right)^2 \right\rangle = \left\langle X^2 \right\rangle - \left\langle X \right\rangle^2 \tag{7}$$

$$\sigma_Y^2 = \left\langle \left( Y - \langle Y \rangle \right)^2 \right\rangle = \left\langle Y^2 \right\rangle - \left\langle Y \right\rangle^2 \tag{8}$$

The variance can be calculated about any number, but it is by subtracting the mean that the minimum variance is obtained. The variance of the difference (Y-X) is given by:

$$\sigma_{(Y-X)}^2 = \left\langle \left( [Y - \langle Y \rangle] - [X - \langle X \rangle] \right)^2 \right\rangle = \sigma_X^2 + \sigma_Y^2 - 2\left\{ \langle XY \rangle - \langle X \rangle \langle Y \rangle \right\} = \sigma_X^2 + \sigma_Y^2 - 2s_{XY} \tag{9}$$

with $s_{XY} = \left\langle \left( Y - \langle Y \rangle \right) \left( X - \langle X \rangle \right) \right\rangle = \langle XY \rangle - \langle X \rangle \langle Y \rangle$ the covariance of $X$ and $Y$. Although we do not in this report calculate the significance of any of these statistics, tests can be applied to determine the significance of many of the statistics described here. Details can be found in Press et al (1992) and some examples of their application to coastal area modelling are given in Hall et al (2000). However there is no fixed dividing line between a significant and an insignificant level of agreement. Willmott (1981) rejects the use of tests of statistical significance, relying on the modeller's knowledge of processes and errors to determine the validity of a correlation. Willmott et al (1985) present a bootstrapping technique as an alternative to the statistical tests of significance in Press et al. (1992). Zambreskey (1989) simply presents the number of points used to calculate each set of statistics. Modellers and users of results will treat examples of validations with more points as being more reliable than validations with only a few.

The average difference between measurements and predictions is given by the Root-Mean-Square Error (RMSE):

$$RMSE = \left\langle \left( Y - X \right)^2 \right\rangle^{1/2} \tag{10}$$

Understanding the lowering of beaches in front of coastal defence structures, Phase 2
Improved predictors for wave-induced scour at seawalls

HR Wallingford

The RMSE can further be split into systematic and unsystematic parts using an ordinary least squares regression of predicted on observed variable. This method fits a straight line ($\hat{Y} = a_{ls} + b_{ls}X$) to the data thereby assuming that there will be a linear relationship between predicted and observed points and that all the error is in the prediction (i.e., the observations are assumed to be error-free). This is never the case in reality, but the relative simplicity of the method means that it is an attractive choice when measured errors are low. (A method of fitting a straight line to data with errors in measurements and predictions is given in Press et al, 1992 §15.3.) In ordinary least squares fitting an error function $\chi^2$ is defined and minimised.

The systematic Root-Mean-Square error, $RMSE_s$, is a measure of how far the best-fit line is from the ideal line ($Y = X$) and is given by

$$RMSE_s = \left\langle \left( \hat{Y} - X \right)^2 \right\rangle^{1/2} \tag{11}$$

Moreover the unsystematic Root-Mean-Square error, $RMSE_u$, is a measure of the scatter of the data about the best-fit line given by

$$RMSE_u = \left\langle \left( \hat{Y} - Y \right)^2 \right\rangle^{1/2} \tag{12}$$

The systematic root-mean-square error may be further broken down into additive, proportional and covariance terms but this represents an unnecessary complication in most circumstances. Note that partitioning the root mean square error into systematic and unsystematic parts represents a complete partitioning of the error as shown by Equation 13.

$$RMSE^2 = RMSE_s^2 + RMSE_u^2 = \sigma_{(Y-X)}^2 + bias^2 \tag{13}$$

The second equality in (13) shows that it is not necessary to quote $RMSE$, $Bias$ and the variance in the difference as any two will be sufficient to derive the third. A graphical presentation of predicted against measured value, with the least squares best-fit line ($\hat{Y} = a_{ls} + b_{ls}X$) included was used to demonstrate the predictor performance. It is not however sufficient to rely on a graphical presentation as the eye can mislead, the error statistic therefore provide a quantitative measure of tendency and deviation.

## 4.2    BEST FIT EQUATIONS FOR TOE SCOUR

The best-fit equations for toe scour depth are given in Equations 14 and 15, which have the break point at $h_t/L_m = 0.0157$.

$$\frac{S_t}{H_s} = \left( 35 \frac{h_t}{L_m} + 0.53 \right)^{1.25} - 0.302 \qquad h_t/L_m \leq 0.0157 \tag{14}$$

$$\frac{S_t}{H_s} = 42 \left( \frac{h_t}{L_m} \right)^2 - 15 \frac{h_t}{L_m} + 1.03 \qquad h_t/L_m > 0.0157 \tag{15}$$

The best-fit lines are shown in Figure 21, with the error statistics given in Table 6. Plots of predicted versus observed scour depths are given in Figure 22. In Table 6 LHS denotes $h_t/L_m$ values below breakpoint, while RHS denotes values above.

Understanding the lowering of beaches in front of coastal defence structures, Phase 2
Improved predictors for wave-induced scour at seawalls

HR Wallingford
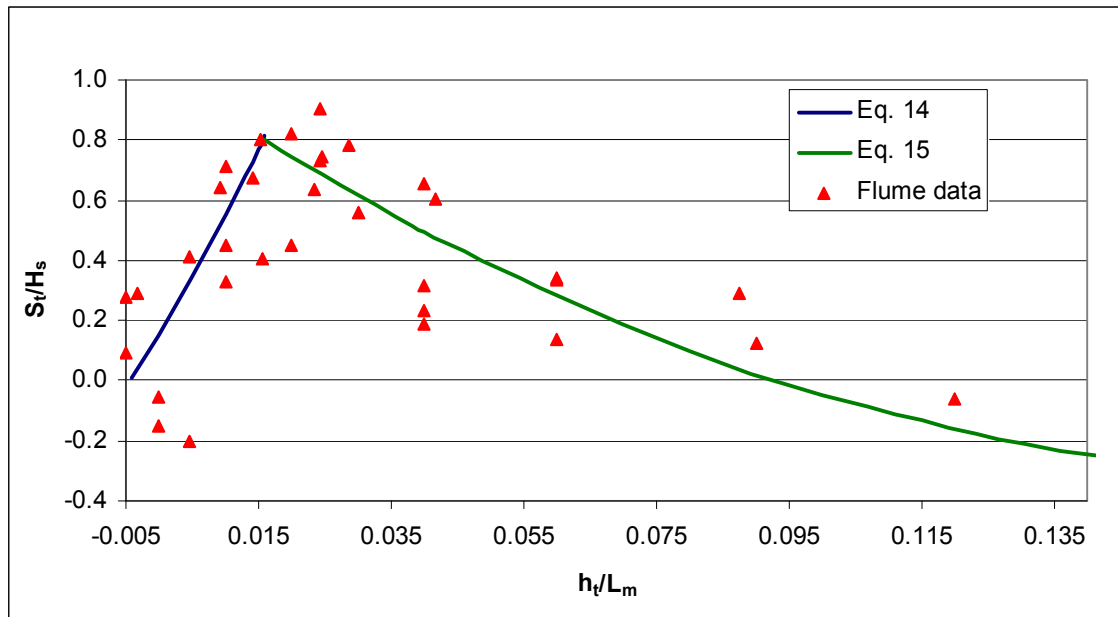
*Figure 21    Best fit equations plotted on graph of $S_t/H_s$ versus $h_t/L_m$ for vertical seawalls*

*Table 6        Error statistics from best-fit lines*

| | RMSE$_S$ | | RMSE$_U$ | | Bias | Bias | RMSE | RMSE |
|---|---|---|---|---|---|---|---|---|
| BP | LHS | RHS | LHS | RHS | LHS | RHS | LHS | RHS |
| 0.0157 | 0.053 | 0.060 | 0.240 | 0.156 | 0.000 | -0.004 | 0.246 | 0.167 |
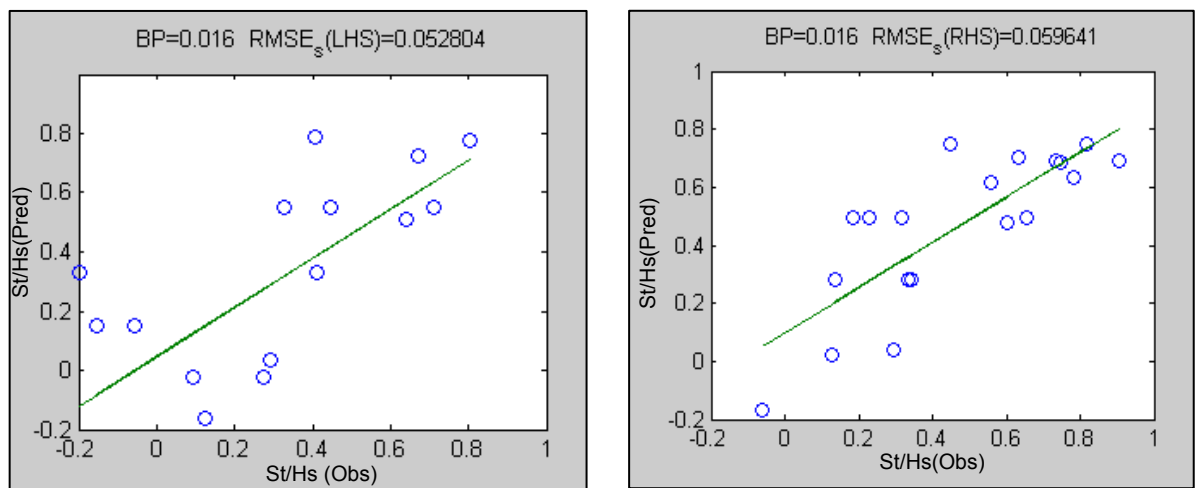


*Figure 22    Predicted versus observed St/Hs with best-fit lines used to separate systematic from unsystematic errors*

Figure 21 shows that Equations 14 and 15 reproduce the form of the relationship between scour depth and relative toe depth. Both low (LHS) and high (RHS) ranges of relative depth have zero bias and relatively low systematic errors (of 0.053 and 0.06 respectively) indicating that the equations are close to the correct form. They both have considerably higher unsystematic errors, which represent the magnitude of the scatter about the best fit lines in Figure 22. This can be reduced by reducing errors in undertaking the experiments or by structurally improving the form of the predictor to include factors not included in Equations 14 and 15.

Understanding the lowering of beaches in front of coastal defence structures, Phase 2
Improved predictors for wave-induced scour at seawalls

HR Wallingford

## 4.3    BEST FIT EQUATIONS FOR MAXIMUM SCOUR

The best-fit equations for maximum scour depth are given in Equations 16 and 17, which have the break point at $h_t/L_m = 0.013$.

$$\frac{S_{max}}{H_s} = \left(35 \frac{h_t}{L_m} + 0.53\right)^{1.12} - 0.12 \qquad h_t/L_m \leq 0.013 \qquad (16)$$

$$\frac{S_{max}}{H_s} = 42 \left(\frac{h_t}{L_m}\right)^2 - 15 \frac{h_t}{L_m} + 1.055 \qquad h_t/L_m > 0.013 \qquad (17)$$

The best-fit lines are shown in Figure 23, with the error statistics given in Table 7. Plots of predicted versus observed scour depths are given in Figure 24.
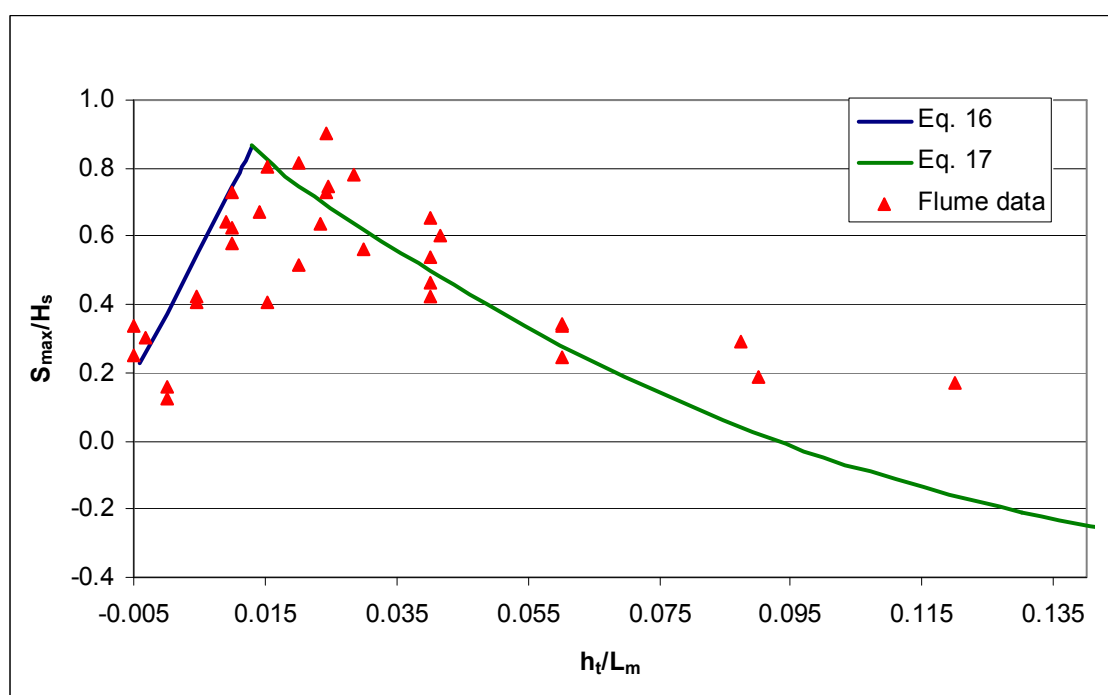


*Figure 23    Best fit equations plotted on graph of $S_{max}/H_s$ versus $h_t/L_m$ for vertical seawalls*

*Table 7        Error statistics for maximum scour depth*

| BP | RMSE$_S$ | | RMSE$_U$ | | Bias | Bias | RMSE | RMSE |
|---|---|---|---|---|---|---|---|---|
| | LHS | RHS | LHS | RHS | LHS | RHS | LHS | RHS |
| 0.013 | 0.053 | 0.010 | 0.173 | 0.160 | 0.000 | -0.006 | 0.181 | 0.160 |

The maximum scour depth predictions are similar to the toe scour predictions. Again there is zero bias and there are low systematic errors, with considerably higher unsystematic errors.

Equations 14 to 17 have a low systematic error and relatively low unsystematic error, but have no basis in physics or our understanding of the processes. For example, if anyone was unwise enough to extrapolate Equations 15 or 17 to significantly deeper water they would get some odd results. The scour depths should tend to zero in deep water and the maximum scour depth

Understanding the lowering of beaches in front of coastal defence structures, Phase 2
Improved predictors for wave-induced scour at seawalls

HR Wallingford

should be zero or positive at all relative depths, whereas Equations 16 and 17 become negative even within the range of data used to create the best fit curves.
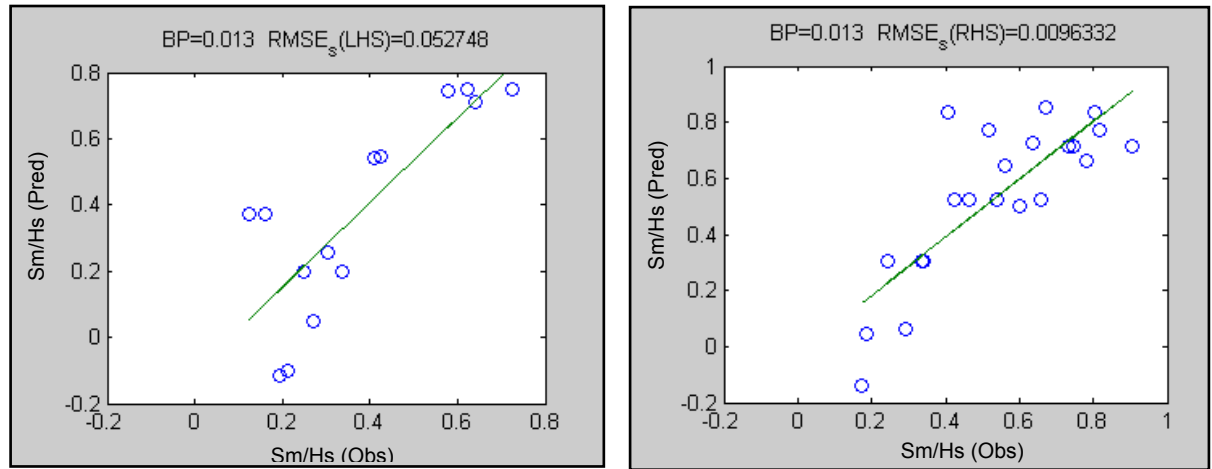


*Figure 24   Predicted versus observed $S_{max}/H_s$ with best-fit lines used to separate systematic from unsystematic errors*

## 4.4    SIMPLIFIED EQUATIONS FOR TOE SCOUR

A new set of best-fit equations were calculated by Andy Pearce based on the following criteria:

1) The equations are relatively simple with fewer fitted coefficients;
2) The toe water depth has been corrected for setup using Holman and Sallenger (1985) where $h_t/L_m \leq 0$.
3) At the break points both equations intersect and produce relative scour depths of $S/H_s \leq 1$, a well known rule of thumb for scour prediction;
4) The predicted scour depth tends towards zero for high relative water depths; and
5) The systematic RMS error for both equations is around 0.1.

Hollman and Sallenger's (1985) expression for the maximum set-up, $\overline{\eta}_{max}$, that would occur on a natural beach is given in Equation 18, where both the wave height and wavelength (in the Iribarren number, Ir) are calculated in deep water but the beach slope is calculated at breaking.

$$\overline{\eta}_{max} = 0.45 H_s \, \text{Ir} = 0.45 \tan(\alpha)\sqrt{H_s L_p} \tag{18}$$

Equation 18 was only applied for cases where $h_t/L_m \leq 0$ as the set-up is a maximum at the shoreline and decreases to the breaker line, where set-down will occur. This relatively simple approach was adopted to see if this change made a difference to the results. In practice there will be an interaction between the incident and reflected waves so parameterisations of setup derived for the open coast may not be particularly accurate.

The best-fit equations for toe scour depth are given in Equations 19 and 20, which have the break point at $h_t^*/L_m = 0.018$, where $h_t^*$ is the toe depth including setup for $h_t/L_m \leq 0$.

$$\frac{S_t}{H_S} = \left(50 \frac{h_t^*}{L_m}\right) \qquad\qquad h_t^*/L_m \leq 0.018 \tag{19}$$

Understanding the lowering of beaches in front of coastal defence structures, Phase 2
Improved predictors for wave-induced scour at seawalls

HR Wallingford

$$\frac{S_t}{H_s} = \frac{0.014}{\sinh\left(h_t^*/L_m\right)^{1.05}} \qquad h_t^*/L_m > 0.018 \qquad\qquad (20)$$

The best-fit lines are shown in Figure 25, with the error statistics given in Table 8. Plots of predicted versus observed scour depths are given in Figure 26. In Table 8 LHS denotes $h_t/L_m$ values below breakpoint, while RHS denotes values above.
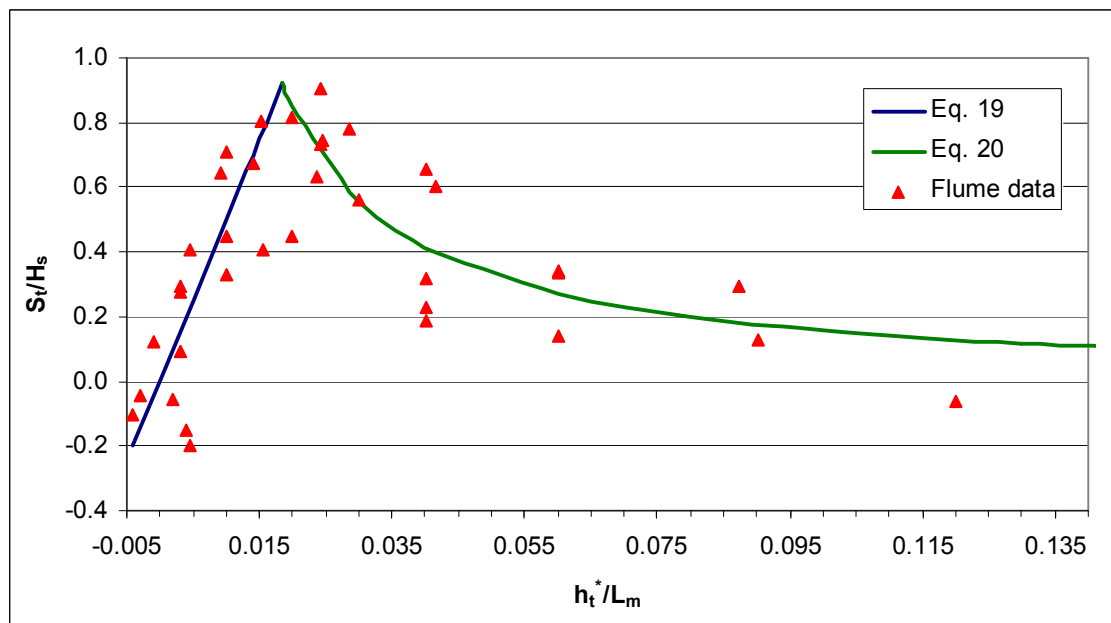


*Figure 25    Simplified best fit lines plotted on graph of $S_t/H_s$ versus $h_t/L_m$*

*Table 8        Error statistics for simplified toe scour equations*

|  | RMSE$_S$ | | RMSE$_U$ | | Bias | Bias | RMSE | RMSE |
|---|---|---|---|---|---|---|---|---|
| BP | LHS | RHS | LHS | RHS | LHS | RHS | LHS | RHS |
| 0.018 | 0.088 | 0.095 | 0.184 | 0.138 | 0.021 | 0.009 | 0.204 | 0.168 |
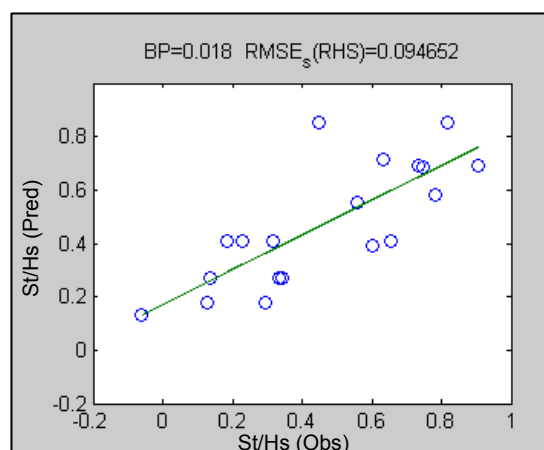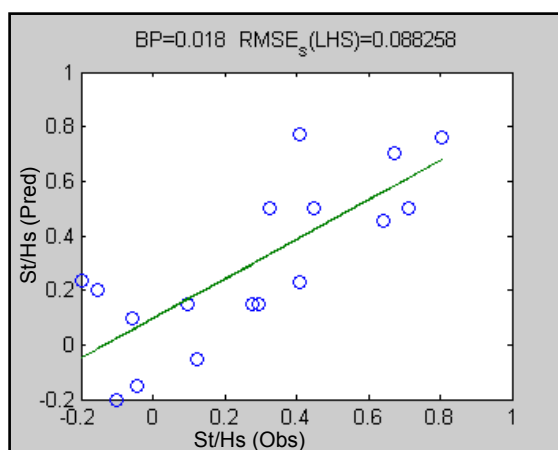


*Figure 26    Predicted versus observed St/Hs using Equations 19 and 20*

Understanding the lowering of beaches in front of coastal defence structures, Phase 2
Improved predictors for wave-induced scour at seawalls

HR Wallingford

## 4.5    SIMPLIFIED EQUATIONS FOR MAXIMUM SCOUR

A new set of best-fit equations for maximum scour were calculated by Andy Pearce based on the criteria used in Section 4.4. The best-fit equations for maximum scour depth are given in Equations 21 and 22, which have the break point at $h_t^*/L_m = 0.016$, where $h_t^*$ is the toe depth including setup given by Equation 18 for $h_t/L_m \leq 0$.

$$\frac{S_{max}}{H_S} = \left(35\frac{h_t^*}{L_m} + 0.40\right)^2 \qquad h_t^*/L_m \leq 0.016 \qquad (21)$$

$$\frac{S_{max}}{H_s} = \frac{0.036}{\sinh\left(h_t^*/L_m\right)^{0.80}} \qquad h_t^*/L_m > 0.016 \qquad (22)$$

The best-fit lines are shown in Figure 27, with the error statistics given in Table 9. Plots of predicted versus observed scour depths are given in Figure 28. In Table 9 LHS denotes $h_t/L_m$ values below breakpoint, while RHS denotes values above.
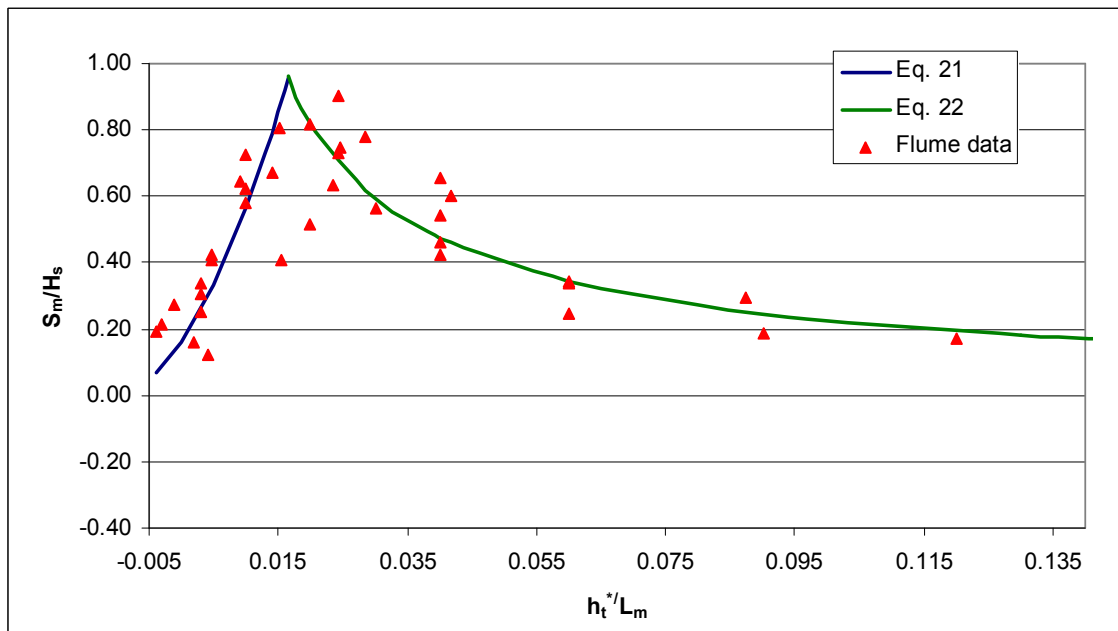


*Figure 27    Simplified best fit lines plotted on graph of $S_m/H_s$ versus $h_t^*/L_m$*

*Table 9        Error statistics for simplified maximum scour equations*

|       | RMSE$_S$ |       | RMSE$_U$ |       | Bias   | Bias   | RMSE  | RMSE  |
|-------|-------|-------|-------|-------|--------|--------|-------|-------|
| BP    | LHS   | RHS   | LHS   | RHS   | LHS    | RHS    | LHS   | RHS   |
| 0.016 | 0.012 | 0.054 | 0.155 | 0.101 | -0.011 | -0.011 | 0.155 | 0.115 |

Understanding the lowering of beaches in front of coastal defence structures, Phase 2
Improved predictors for wave-induced scour at seawalls

HR Wallingford
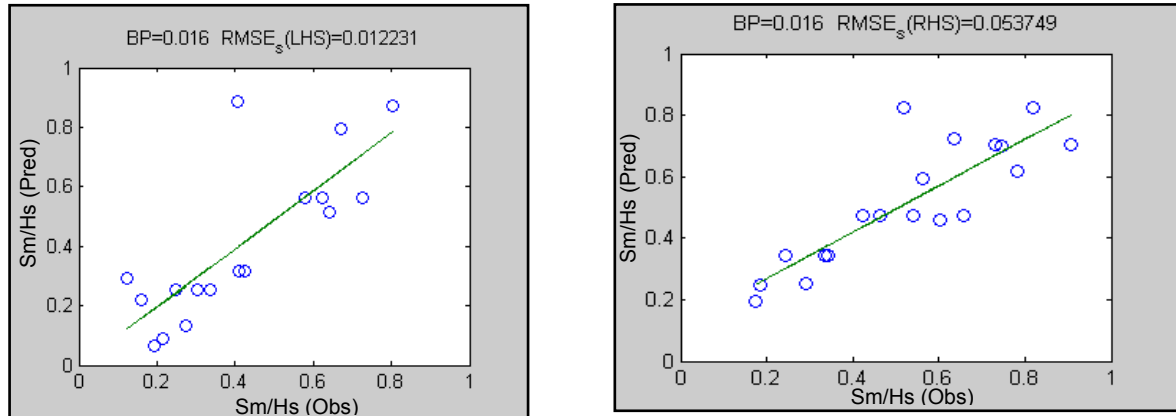
*Figure 28    Predicted versus observed scour depth using Equations 21 and 22*

Equations 19 to 22 have fewer fitted coefficients than equations 14 to 18 but do include the calculated wave setup for $h_t/L_m \leq 0$. They produce lower systematic error and unsystematic errors for maximum scour prediction but higher bias. For toe scour the simplified predictors have higher systematic error and higher bias, but lower unsystematic error. A comparison of the total RMS error, RMSE for the four cases shows that Equations 14 and 15 for toe scour have RMSE = 0.25 and 0.17, while Equations 19 and 20 have RMSE = 0.20 and 0.17. Equations 16 and 17 for maximum scour have RMSE = 0.18 and 0.16, compared to equations 21 and 22 which have RMSE = 0.16 and 0.12. Incorporating a relatively simple equation for those datapoints most affected by setup has allowed a low RMS error to be achieved while simplifying the equations for toe scour and maximum scour at a vertical seawall on a sand beach. Equations 19 and 20 are therefore recommended for calculating toe scour, while Equations 21 and 22 are recommended for calculating the maximum scour depth. In each case the RMS error can be used to estimate the uncertainty in the prediction.

## 4.6    CONSERVATIVE ESTIMATE OF TOE SCOUR DEPTH

Sutherland et al. (2006a) fitted a conservative toe scour depth curve to a combined dataset that included field results from Blackpool and Southbourne, reproduced as Figure 29. The equation was fitted to the maximum value of relative toe scour depth, $S_{tmax}$, for each range of relative water depth. This is intended to provide a conservative estimate of the toe scour depth and was fitted by eye to the data. Note that the version of this equation given in Sutherland et al. (2006a) is not correct. The correct version is given in Equation 23, which is considered a reasonable predictor of the maximum toe scour depth in sand likely to be encountered for a given water depth at the structure toe, $h_t$, and offshore linear theory mean wavelength, $L_m$. Setup is not included in this method.

$$\frac{S_{t\,max}}{H_s} = 4.5e^{-8\pi(h_t/L_m + 0.01)}\left(1 - e^{-6\pi(h_t/L_m + 0.01)}\right) \qquad (23)$$

The tests were within the following ranges: $-0.013 \leq h_t/L_m \leq 0.18$ and $0 \leq Ir \leq 0.43$. Equation 23 should only be applied within those ranges and users should note that some parts of those ranges were covered more thoroughly than others. The maximum scour depth appears to decrease as beach slope decreases for the same offshore wave conditions. Moreover, the maximum scour depth seems to occur at larger relative depths for lower beach slopes. However, neither phenomenon has been well validated and hence they are not calculated in this method.

Understanding the lowering of beaches in front of coastal defence structures, Phase 2
Improved predictors for wave-induced scour at seawalls

HR Wallingford
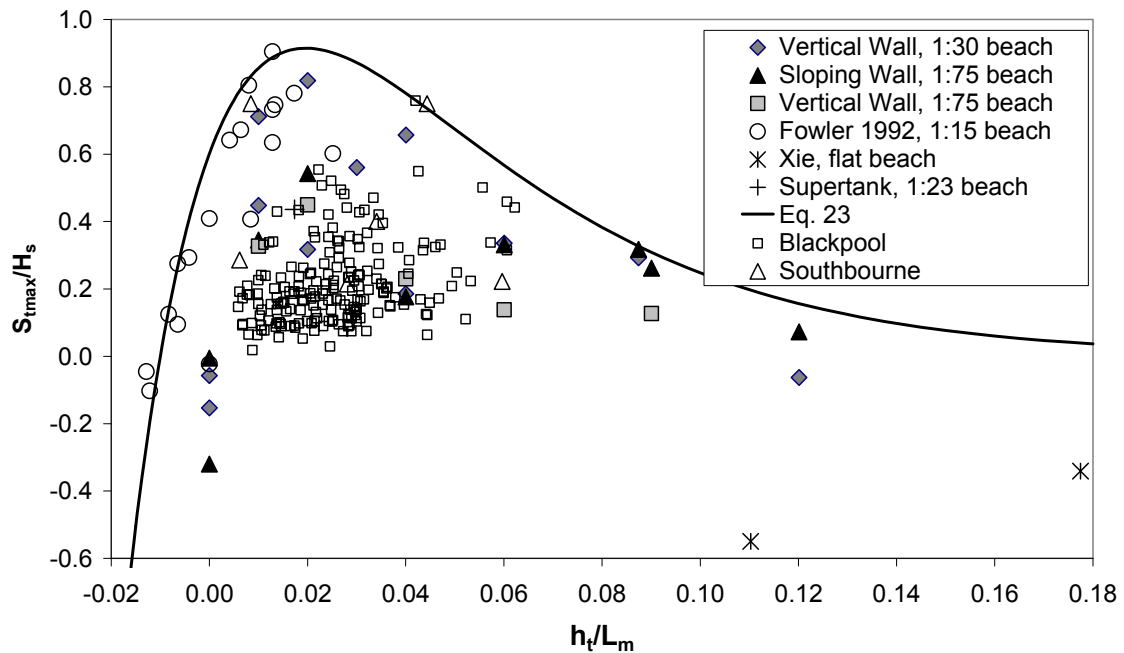


*Figure 29    Maximum scour depth predictor after Sutherland et al., 2006a*

## 4.7    SINGLE EQUATION FOR AVERAGE TOE SCOUR DEPTH

An equation of the form of Equation 23 was fitted to the data (this time including the Holman and Sallenger setup for $h_t/L_m \leq 0$) to provide a best estimate of the scour depth as a function of relative depth. The fitting was first performed to minimise the systematic Root-Mean-Square error, $RMSE_S$, to give Equation 24.

$$\frac{S_t}{H_s} = 6.5e^{-6k_m h_t^*}\left(1 - e^{-3.03k_m h_t^*}\right) - 0.194 \tag{24}$$

Equation 24 is plotted with the laboratory flume data in Figure 30, which shows that it fits the form of the data reasonably well, but tends to a negative value for very deep water. The data is shown plotted by beach slope. Figure 31 shows the predicted non-dimensional scour depths plotted against the observed, with the best-fit straight line plotted, which shows that the systematic error has been almost completely eliminated. The error statistics are given in Table 10. The Root-Mean-Square Error, RMSE, is higher than for the examples given in Sections 4.1.2 to 4.1.5 where 2 equations are used, but the fact that the systematic error is effectively zero implies that the variation of scour depth with relative depth has been reasonably well reproduced. The remaining error can be ascribed to scatter in the experimental data and to factors other than relative depth influencing the scour depth. Section 3.2 illustrated that it is unreasonable to expect relative depth to be the only controlling parameter.

A second fit to the data was then performed to minimise the RMS Error, which produced Equation 25. The error statistics for Equation 25 are also given in Table 10, while Equation 25 is plotted on Figure 30. Figure 30 shows that equation 25 has a lower peak value for toe scour, tends to a value of zero for high relative depths and tends to lower values than Equation 24 for negative $h_t/L_m$. Table 10 shows that the RMS error, RMSE, is lower than for equation 24, but that it is composed of systematic as well as unsystematic errors. Figure 32 shows the predicted

Understanding the lowering of beaches in front of coastal defence structures, Phase 2
Improved predictors for wave-induced scour at seawalls

HR Wallingford

non-dimensional scour depths plotted against the observed, with the best-fit straight line, which shows the systematic error.

$$\frac{S_t}{H_s} = 10e^{-7.25k_m h_t^*}\left(1 - e^{-1.35k_m h_t^*}\right)$$

(25)
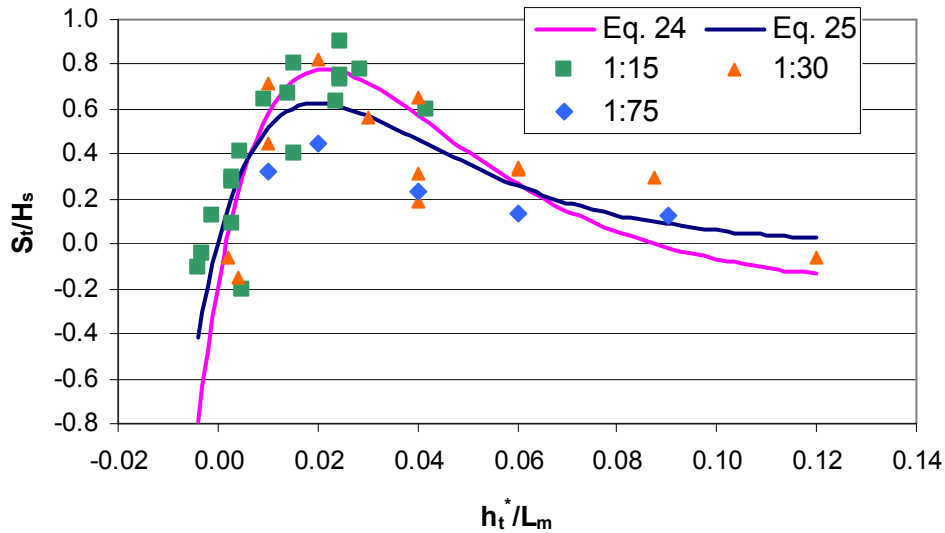


*Figure 30    Equations 24 and 25 for toe scour plotted with flume data*

*Table 10    Error statistics for Equations 24, 25, 26 and 27*

| Equation | $RMSE_S$ | $RMSE_U$ | Bias | RMSE | Best fit line slope | Best fit line intercept |
|---|---|---|---|---|---|---|
| 24 | 0.000 | 0.254 | 0.000 | 0.254 | 0.999 | 0.001 |
| 25 | 0.107 | 0.169 | -0.014 | 0.200 | 0.652 | 0.116 |
| 26 | 0.000 | 0.222 | 0.000 | 0.222 | 1.000 | 0.000 |
| 27 | 0.000 | 0.239 | 0.000 | 0.239 | 1.000 | 0.000 |
| 28 | 0.000 | 0.226 | 0.000 | 0.226 | 0.999 | 0.000 |

Understanding the lowering of beaches in front of coastal defence structures, Phase 2
Improved predictors for wave-induced scour at seawalls

HR Wallingford
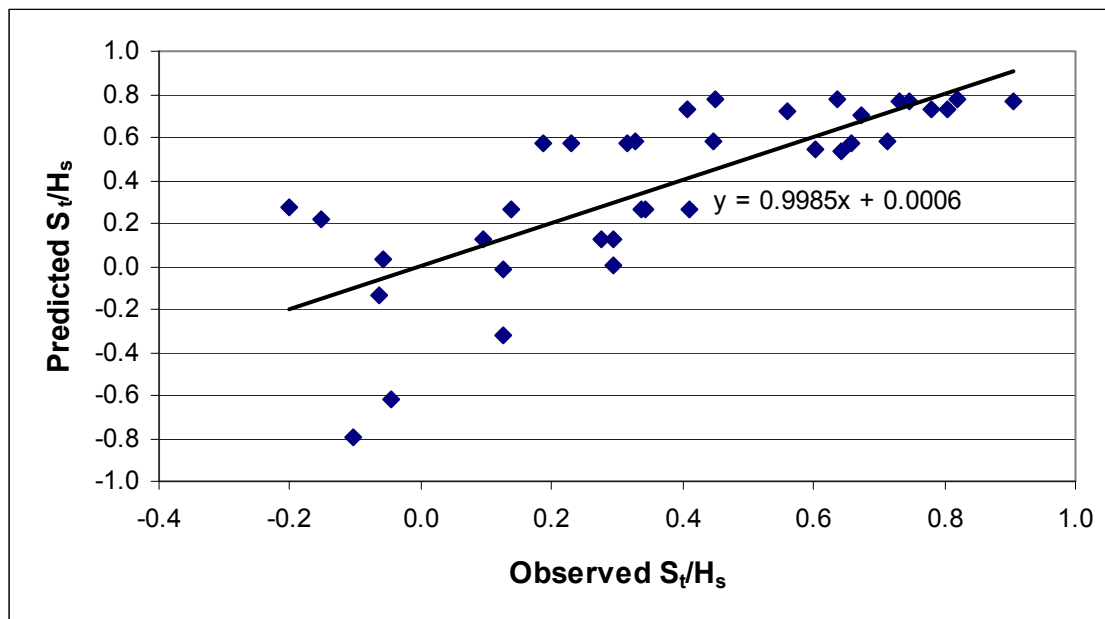
*Figure 31    Predicted against observed toe scour depth using Equation 24*
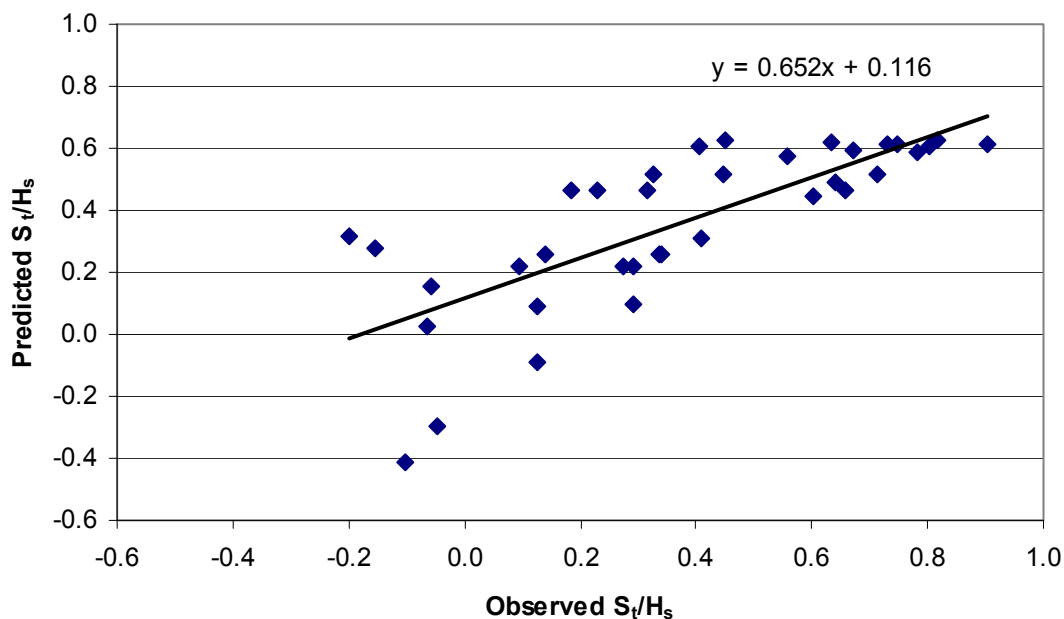


*Figure 32    Predicted against observed toe scour depth using Equation 25*

Equation 25 is simpler than Equation 24 and has a lower overall RMS error, but it under-predicts the highest measured scour depths and contains a systematic error.

Equation 24 can be improved with additional terms.  In order to see which terms were important, the residual scour depth was calculated by subtracting the predicted non-dimensional scour depth (using Equation 24) from the best-fit line shown in Figure 31 (which is effectively the same as the measured non-dimensional scour depth).  The residual scour depth is the scatter of the predictions about the best-fit line.  Figures 33 and 34 show the residual scour depth

Understanding the lowering of beaches in front of coastal defence structures, Phase 2
Improved predictors for wave-induced scour at seawalls

HR Wallingford

plotted against the beach slope, $\tan(\alpha)$, and $h_t/H_s$ respectively, which are both factors that influence scour depth.
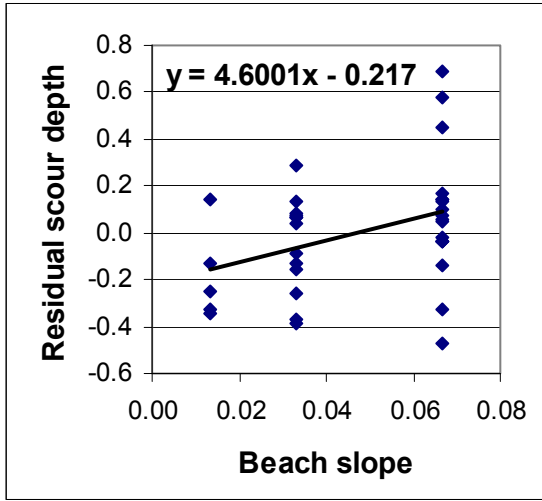


*Figure 33   Residual scour depth against beach slope*
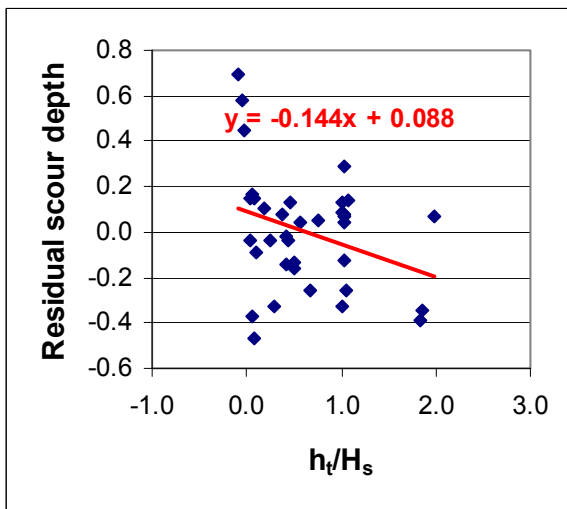


*Figure 34   Residual scour depths against relative toe depth*

The best-fit lines in Figures 33 and 34 indicate that there is a dependence of scour depth on both beach slope and relative toe depth, although there is more scatter than trend. Incorporating terms derived from Figures 33 and 35 into the formula for toe scour depth gives Equations 26 and 27 respectively. The error statistics from Equations 26 and 27 are also given in Table 10.

$$\frac{S_t}{H_s} = 6.15e^{-6k_m h_t^*}\left(1 - e^{-3.k_m h_t^*}\right) - 0.37 + 4.49\tan(\alpha) \tag{26}$$

$$\frac{S_t}{H_s} = 6.34e^{-5.5k_m h_t^*}\left(1 - e^{-3k_m h_t^*}\right) - 0.113 - 0.182\left(\frac{h_t}{H_s}\right) \tag{27}$$

An alternative approach to incorporating the bed slope is given by Equation 28, where a function of the beach slope, $\alpha$ (in radians) acts as a multiplier, rather than an additive term. The

Understanding the lowering of beaches in front of coastal defence structures, Phase 2
Improved predictors for wave-induced scour at seawalls

HR Wallingford

predicted curves from Equation 28 are shown in Figure 35, while the predicted relative toe scour depths are plotted against the observed values in Figure 36. In Figure 35, 'O 1:N' represents the observed values for an initial beach slope of 1:N, while 'P 1:N' represents the predicted curve for a beach slope of 1:N.

$$\frac{S_t}{H_s} = 6.8\left(0.207\ln(\alpha)+1.51\right)e^{-5.85k_mh_t}\left(1-e^{-3k_mh_t}\right)-0.137 \qquad [-0.04 \leq h_t/L_m \leq 0.12] \quad (28)$$
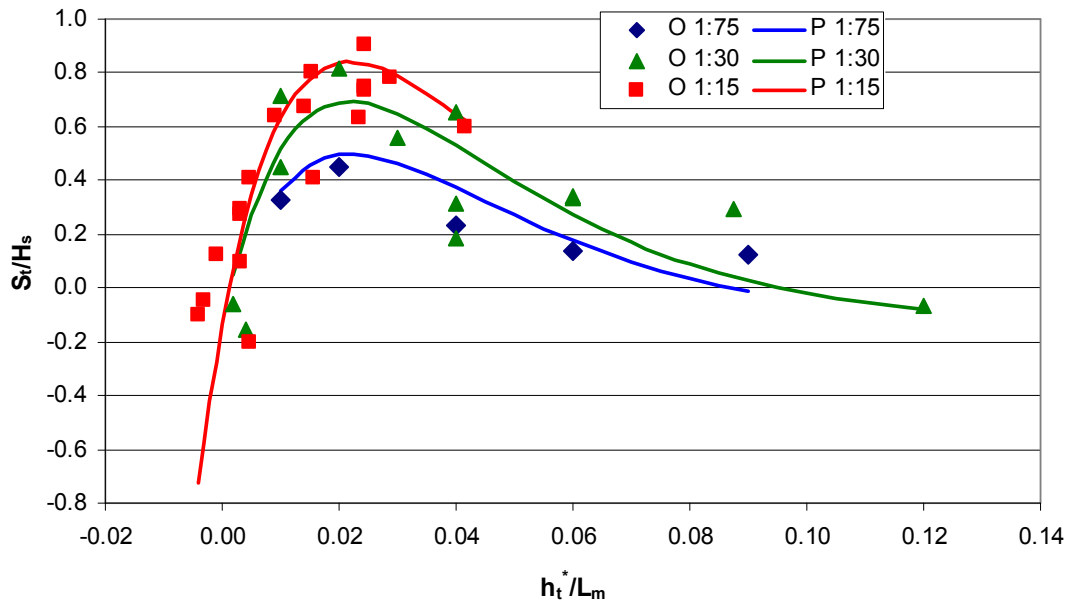
Figure 35    *Predicted scour depths as a function of relative depth and beach slope (Eq. 28) plotted with flume data*
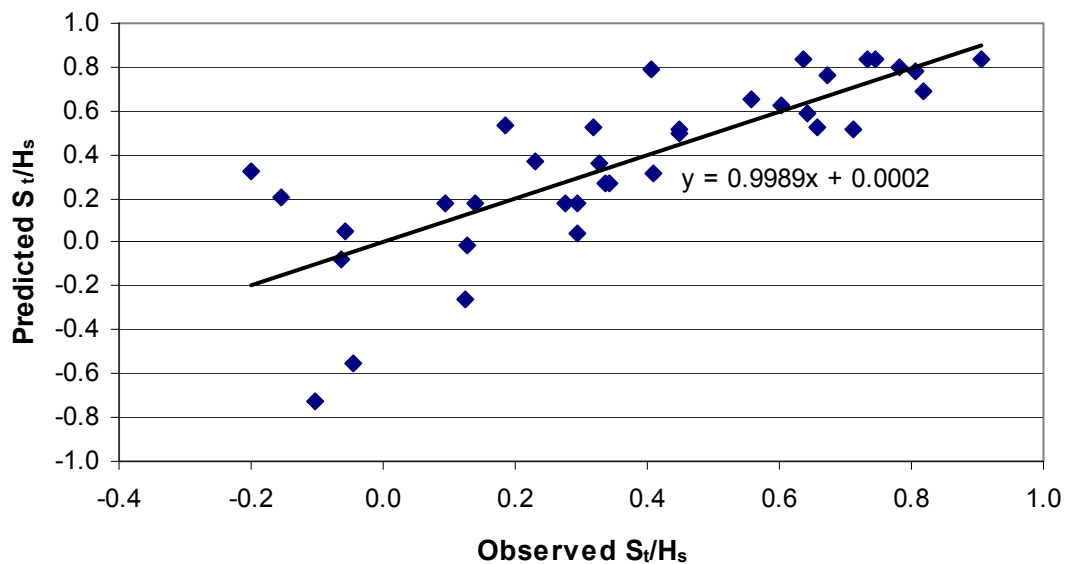
Figure 36    *Predicted against observed toe scour depth using Equation 28*

Understanding the lowering of beaches in front of coastal defence structures, Phase 2
Improved predictors for wave-induced scour at seawalls

HR Wallingford

Equations 26, 27 and 28 all give zero bias and systematic RMS error, a best-fit line with a slope of (close to) 1 and intercept of zero and a slightly lower unsystematic RMS error than equation 24. However, the RMS error, RMSE, remains higher than those given by Equation 25, or indeed Equations 19 and 20. Equation 26 gives a slightly lower unsystematic RMS error than Equation 28, but has predictions that are separated by a constant amount for different beach slopes. The author favours Equation 28 as Equation 26 under predicts the highest relative scour depths while Equation 28 includes terms for both relative depth and beach slope and its RMSE is relatively low.

# 5.   Limitation of medium scale flume experiments

The large majority of the medium scale laboratory flume tests included in this report using irregular period waves had incident significant wave heights between about 0.18m and 0.25m (see Tables 2 to 5). This limited range of wave heights was used as the waves needed to be high enough to generate suspended sediment transport and medium scale flumes are not capable of generating significant wave heights much greater than this. This means that the effect of wave height on scour depth has not been fully investigated and whilst the scaling of scour depth with offshore significant wave height is reasonable it has not been tested outside a limited range.

The best-fit scour equations predict a maximum scour depth at a relative depth of $h_t/L_m \approx 0.02$. At the same time observation of the processes and the resulting scour depths suggests that the greatest toe scour depths occur when waves break directly onto the seawall. In the HR Wallingford (2006b) flume experiment this occurred for water depths of $h_t \approx H_s$. If significantly larger wave heights were used with waves of the same period these two criteria for generating the greatest scour depths would not be met simultaneously and it would be possible to develop a scour predictor with a higher level of confidence.

Fowler (1992) used a median grain diameter of 0.13mm while HR Wallingford (2006b) used 0.11mm sand. Therefore the effect of wave height to grain size (a measure of sediment mobility) could benefit from further investigation. Moreover, the bed profiles in the medium scale tests show the presence of ripples formed during the tests. These ripples would be washed out by wave action at a larger scale and their presence may affect the final scour depth.

The Fowler (1992) and HR Wallingford (2006) flume tests utilised a smooth planar initial sand bed to provide a consistent level for comparison between tests. The development of an equilibrium profile in front of the wall is likely to affect the wave breaking and hence scour at the wall. These tests therefore represent a situation in the field where low beach volumes prevent an equilibrium beach profile from forming.

It is therefore recommended that a structured series of large scale laboratory tests on wave-induced scour in front of a vertical coastal structure be carried out[1] to address the limitations identified (on the range of wave heights and grain sizes) and provide added confidence in the scour predictors presented here.

---

[1] The EU Integrated Infrastructure Initiative, HYDRALAB, will provide limited access to large-scale experimental facilities, including three large wave flumes (GWK, Delta flume and CIEM flume) between 2007 and 2010, based on the selection of grant proposals by a User Selection Panel. A successful application would pay for the hire of the facility, travel and accommodation, but not staff time for planning, testing, analysis and interpretation.

Understanding the lowering of beaches in front of coastal defence structures, Phase 2
Improved predictors for wave-induced scour at seawalls

HR Wallingford

# 6. Conclusions

An extensive literature review (Sutherland et al., 2003) and assessment of existing datasets (HR Wallingford, 2006a) have been used to identify laboratory test datasets that include measurements of toe scour and maximum wave-induced scour in front of vertical or sloping seawalls with wave heights sufficiently high to generate suspended sediment transport. A set of new laboratory experiments was then planned (HR Wallingford, 2006a) to address some of the shortcomings identified. The new test programme was then executed and documented (HR Wallingford, 2006b) and interpreted (Pearce et al., 2006, Sutherland et al., 2006b).

The combined laboratory dataset was then used to derive Equations 19 and 20 (representing low and high values of relative water depth) for toe scour depth and Equations 21 and 22 for the maximum scour depth. Statistical analysis gave a Root-Mean-Square error in the predicted values of relative scour depth of about 0.17. It became clear that relative toe depth is not the only parameter governing toe scour and the influence of a number of factors has been discussed (in Sections 2.3 to 2.7). Equation 24 was derived as a single equation to calculate toe scour depth as a function of $h_t/L_m$. It was then expanded into Equation 28 which takes beach slope as well as relative toe depth into account. This predictor provides significant additional predictive capability for seawall scour in sand beaches.

Limitations of the medium-scale flume tests have been identified, in terms of the range of wave heights and bed sediments tested. A set of large scale flume tests is therefore recommended to discriminate the effect of wave height and sediment size on scour depth. Partial funding for such experiments is potentially available through the present round of the Access to Large Scale Facilities programme of the EU Integrated Infrastructure Initiative, HYDRALAB.

# 7. References

Barnett, M., 1987. Laboratory study of the effects of a vertical seawall on beach profile response. Report 87/005, Coastal and Oceanographic Engineering department, University of Florida, Gainsville, Fl., USA.

Battjes, J.A., 1974. Surf similarity. *Proceedings of the 14th Int Conf on Coastal Engineering*, ASCE, pp. 466-480.

Chesnutt, C.B. and Schiller, R.E., 1971. *Scour of simulated Gulf Coat sand beaches due to wave action in front of sea walls and dune barriers*. COE Report No. 139. TAMU-SG-71-207. Texas A&M University, College Station, TX.

Carter, T.G., Liu L.-F.P. and Mei, C.C., 1973. Mass transport by waves and offshore sand bedforms. *ASCE Journal of Waterway, Port, Coastal and Ocean Engineering*, 99(WW2): 165-184.

Fowler, J.E., 1992. *Scour problems and methods for prediction of maximum scour at vertical seawalls.* Technical Report CERC-92-16, U.S. Army Corps of Engineers, Waterways Experiment Station, 3909 Halls Ferry Road, Vicksburg, MS.

Hall, L.J., Sutherland, J., Baugh, J.V. and T.J. Chesher, 2000. Validation of PISCES using data from Teignmouth Pilot Experiment. HR Wallingford Report TR112. December 2000.

Understanding the lowering of beaches in front of coastal defence structures, Phase 2
Improved predictors for wave-induced scour at seawalls

HR Wallingford

Holman, R.A. and Sallenger, A.H., 1985. Set-up and swash on a natural beach. J Geophys. Res., 90, 945 – 953.

HR Wallingford, 2005a. Beach lowering and recovery at Southbourne (2005). HR Wallingford Technical Note CBS0726/01, prepared for Defra project FD1927.

HR Wallingford, 2005b. Scour monitor deployment at Blackpool. HR Wallingford Technical Note CBS0726/04, prepared for Defra project FD1927.

HR Wallingford, 2006a. Design of physical model scour tests. HR Wallingford Technical Note CBS0726/02, prepared for Defra project FD1927.

HR Wallingford, 2006b. Medium scale 2D physical model tests of scour at sea walls. HR Wallingford Technical Note CBS0726/06, prepared for Defra project FD1927.

Hughes, S.A & Fowler, J.E., 1991. Wave-induced scour prediction at vertical walls. Proceedings Coastal Sediments, Vol 2 , pp1886-1900.

Kraus, N.C. and Smith, J.M. (editors), 1994. *SUPERTANK Laboratory data collection project. volume 1: Main text*. Technical report CERC-94-3, US Army Corps of Engineers Waterways Experiment Station, Coastal Engineering Research Center, Vicksburg. Miss.

Longuet-Higgins, M.S., 1953. Mass transport in water waves. *Phil. Trans. Roy. Soc., London, series A*, 245: 535-581.

McDougal, W.G. Kraus N. and H. Ajiwibowo, 1986. The effects of seawalls on the beach Part 2: numerical modeling of SUPERTANK seawall tests. *Journal of Coastal Research* Vol 12(3) pp. 702 – 713

O'Donoghue, T., 2001. N type sediment bed response under standing wave. *J. Waterway, Port, Coastal and Ocean Engineering*, 127: 245 – 248.

Pearce, A.M.C., Sutherland, J., Obhrai, C., Müller, G. and Whitehouse, R., 2006. Scour at a seawall – field measurements and physical modelling. Proceedings, *30th Int Conf, Coastal Engineering, 2006*, San Diego (in press).

Powell, K.A. and Lowe, J.P., 1994. The scouring of sediments at the toe of seawalls. In Proceedings Hornafjordur International Coastal Symposium, Iceland. Viggosson, G. (Ed.) pp 749 – 755.

Powell, K. and Whitehouse, R., 1998. The occurrence and prediction of scour at coastal and estuarine structures. In Proceedings 33rd MAFF Conference of River and Coastal Engineers, Keele, UK.

Press, W.H., Teukolsky, S.A., Vetterling, W.T. and Flannery, B.P., 1992. Numerical Recipes in Fortran, second edition. Cambridge University Press.

Smith, J.M., 2003. Surf zone hydrodynamics. Part 2, Chapter 4 of the *Coastal Engineering Manual,* USACE EM 1110-2-1100. INTERNET: available from http://www.usace.army.mil/publications/eng-manuals/em.htm (page accessed 27/09/06).

Soulsby, R.L., 1997. *Dynamics of Marine Sands*. Thomas Telford, London. ISBN 07277 2584 X

Understanding the lowering of beaches in front of coastal defence structures, Phase 2
Improved predictors for wave-induced scour at seawalls

HR Wallingford

Sumer, B.M. and Fredsøe, J., 2000. Experimental study of 2D scour and its protection at a rubble-mound breakwater. *Coastal Engineering*, vol 40. 5-87. Elsevier Science.

Sumer, B.M. and Fredsøe, J., 2002. The mechanics of scour in the marine environment. World Scientific, ISBN 981-02-4930-6, pp 536.

Sutherland, J., Brampton, H., Motyka, G., Blanco, B. and Whitehouse, R., 2003 *Beach lowering in front of coastal structures, research scoping study*. Defra R&D Technical Report FD1916/TR1. ISBN 0-85521-163-6. Available from http://sciencesearch.defra.gov.uk (page accessed 07/09/2006).

Sutherland, J., Brampton, A. and Whitehouse, R., 2006a. Toe scour at seawalls: monitoring, prediction and mitigation. Proceedings, *41st Defra Flood and Coastal Management Conference*, York, pp 3b.01.1 – 3b.01.12

Sutherland, J., Obhrai, C., Whitehouse, R.J.S. and Pearce, A.M.C., 2006b. Laboratory tests of scour at a seawall. *Proceedings, 3rd Int Conf Scour and Erosion,* Amsterdam. A.A. Balkema, CD-ROM.

Willmott, C.J., 1981. On the validation of models. Physical Geography 2(2): 184–194.

Willmott, C.J., Ackleson, S.G., Davis, R.E., Feddema, J.J., Klink, K.M., Legates, D.R. and C.M. Rowe, 1985. Statistics for the evaluation and comparison of models. J Geophysical Research 90(C5): 8995–9005.

Xie, S-L., 1981. *Scouring patterns in front of vertical breakwaters and their influence on the stability of the foundations of the breakwaters*. Department of Civil Engineering, Delft University of Technology, Delft, The Netherlands, 61p.

Xie, S-L., 1985. Scouring patterns in front of vertical breakwaters. Acta Oceanologica Sinica. 4(1): 1153 – 164.

Zambresky, L., 1989. A verification study of the global WAM model, December 1987 – November 1988. GKSS Forschungszentrum Technical Report No. 63.

Understanding the lowering of beaches in front of coastal defence structures, Phase 2
Improved predictors for wave-induced scour at seawalls

HR Wallingford